2014

A Posteriori Error Estimates for Surface Finite Element Methods

Fernando F. Camacho
University of Kentucky, fercamachof@gmail.com

STUDENT AGREEMENT:

I represent that my thesis or dissertation and abstract are my original work. Proper attribution has been given to all outside sources. I understand that I am solely responsible for obtaining any needed copyright permissions. I have obtained needed written permission statement(s) from the owner(s) of each third-party copyrighted matter to be included in my work, allowing electronic distribution (if such use is not permitted by the fair use doctrine) which will be submitted to UKnowledge as Additional File.

I hereby grant to The University of Kentucky and its agents the irrevocable, non-exclusive, and royalty-free license to archive and make accessible my work in whole or in part in all forms of media, now or hereafter known. I agree that the document mentioned above may be made available immediately for worldwide access unless an embargo applies.

I retain all other ownership rights to the copyright of my work. I also retain the right to use in future works (such as articles or books) all or part of my work. I understand that I am free to register the copyright to my work.

REVIEW, APPROVAL AND ACCEPTANCE

The document mentioned above has been reviewed and accepted by the student's advisor, on behalf of the advisory committee, and by the Director of Graduate Studies (DGS), on behalf of the program; we verify that this is the final, approved version of the student's thesis including all changes required by the advisory committee. The undersigned agree to abide by the statements above.

Fernando F. Camacho, Student

Dr. Alan Demlow, Major Professor

Dr. Peter Perry, Director of Graduate Studies

A POSTERIORI ERROR ESTIMATES FOR SURFACE FINITE ELEMENT METHODS

DISSERTATION

A dissertation submitted in partial fulfillment of the requirements for the degree of
Doctor of Philosophy in the Department of Mathematics
at the University of Kentucky
June 2014

by
Fernando Camacho

Lexington, Kentucky

Director: Dr. Alan Demlow..... Professor of Mathematics

Lexington, Kentucky

ABSTRACT OF DISSERTATION

A POSTERIORI ERROR ESTIMATES FOR SURFACE FINITE ELEMENT METHODS

Problems involving the solution of partial differential equations over surfaces appear in many engineering and scientific applications. Some of those applications include crystal growth, fluid mechanics and computer graphics. Many times analytic solutions to such problems are not available. Numerical algorithms, such as Finite Element Methods, are used in practice to find approximate solutions in those cases.

In this work we present L^2 and pointwise a posteriori error estimates for Adaptive Surface Finite Elements solving the Laplace-Beltrami equation $-\triangle_\Gamma u = f$. The two sources of errors for Surface Finite Elements are a Galerkin error, and a geometric error that comes from replacing the original surface by a computational mesh. A posteriori error estimates on flat domains only have a Galerkin component. We use residual type error estimators to measure the Galerkin error. The geometric component of our error estimate becomes zero if we consider flat domains, but otherwise has the same order as the residual one. This is different from the available energy norm based error estimates on surfaces, where the importance of the geometric components diminishes asymptotically as the mesh is refined. We use our results to implement an Adaptive Surface Finite Element Method.

An important tool for proving a posteriori error bounds for non smooth functions is the Scott-Zhang interpolant. A refined version of a standard Scott-Zhang interpolation bound is also proved during our analysis. This local version only requires the interpolated function to be in a Sobolev space defined over an element T instead of an element patch containing T.

In the last section we extend our elliptic results to get estimates for the surface heat equation $u_t - \triangle_\Gamma u = f$ using the elliptic reconstruction technique.

Keywords: Numerical Analysis, Finite Element Methods, Adaptive Refinement, Partial Differential Equations on Surfaces, Laplace Beltrami Operator.

A POSTERIORI ERROR ESTIMATES FOR SURFACE FINITE ELEMENT METHODS

By

Fernando Camacho

Director of Thesis: Alan Demlow

Director of Graduate Studies: Peter Perry

Date: July 30, 2014

To my family: Victor, Vickie and Tabatha Camacho for filling my life with love. A special recognition to my parents Faustino and Leticia for all their love and support.

Acknowledgements

I want to express my sincere gratitude to my advisor Professor Alan Demlow for all his guidance, patience and dedication to help me succeed. He always make himself available to answer my questions and was ready to discuss difficult concepts with me. Without his help and mentoring this dissertation would not have been possible. I feel very fortunate to have such an exceptional advisor.

I also want to thank my committee members Professor Qiang Ye, Professor John Lewis, Professor Cidambi Srinivasan and Professor Charles Lu for taking the time to read this work, for sharing their experience with me and for their comments and advise.

I am very grateful with all the faculty members that influenced me to follow this wonderful path. Professor Quiang Ye, whose Numerical Linear Algebra classes inspired me to chose Numerical Analysis. Professor Jeffrey Ovall, who introduced me to the world of Numerical PDEs and to my advisor Alan Demlow. Professor Changyou Wang for his wonderful lectures and for all the time he spent with me answering questions. I deeply enjoy all the five classes that I took with Professor Wang.

I want to recognize Professor Avinash Sathaye, Professor Edgar Enochs and Professor Uwe Nagel for helping me study for my last preliminary exam. I am in debt with all of them for all their help and encouragement. Professor Peter Perry for all his help and support when I started a second degree outside of the department of Mathematics. Professor James McDonough for sharing his experience with me and

for helping me develop a background in Computational Fluid Dynamics.

Finally to my family, their love is a blessing that makes my life better and helps keep going during the most stressful moments.

This material is based upon work supported by the National Science Foundation under Grant No. DMS-1016094. Any opinions, findings, and conclusions or recommendations expressed in this material are those of the author and do not necessarily reflect the views of the National Science Foundation.

Contents

List of Figures

Chapter 1

Introduction

We present adaptive surface finite element methods (ASFEM) solving elliptic and parabolic partial differential equations (PDEs) on surfaces. The adaptive algorithms are based on the L^2 and pointwise error estimates proved in chapter 3.

1.1 Finite Element Method

The finite element method (FEM) is an important tool in engineering and science used to approximate the solution of a partial differential equation (PDE) over a given domain. It was first developed to solve problems in structural analysis. In 1942 Courant published an article [18] in which he solved the St. Venant's torsion of a hollow square box. In this work he introduced a Rayleigh-Ritz method with piecewise continuous polynomials defined over a triangular mesh to obtain an approximate solution. The name finite element method is attributed to Clough who first used the term in [17] (cf. [37], [47]).

We proceed to state some basic definitions and explain briefly the mechanics of a FEM. The interested reader is directed to [29] and [11] for a more in depth treatment.

Definition. [See [29]] Let $\mathcal{D}$ be a domain in $\mathbb{R}^d$. A **mesh** $\mathcal{T}_h$ of $\mathcal{D}$ is a union of a finite number N of compact, connected Lipschitz domains T_i with non-empty interior such that $\{T_i\}_{i=1}^N$ forms a partition of $\mathcal{D}$, i.e,

$$\bar{\mathcal{D}} = \bigcup_{i=1}^{N} \{T_i\}, \text{ and } \mathring{T}_j \bigcap \mathring{T}_i = \emptyset \text{ for } i \neq j.$$

The subsets T are called the mesh **elements**. The subscript h on $\mathcal{T}_h$ refers to the level of refinement of the mesh. For notational ease we will drop the sub-index h and refer to the mesh simply as $\mathcal{T}$ unless there is danger of confusion.

Definition. A mesh is said to be **conforming** if for any $T_i, T_j \in \mathcal{T}$ their intersection is either a common edge or vertex of both elements.

Definition. The **element diameter** h_T is the diameter of the smallest ball containing an element T of $\mathcal{T}$.

Definition. The **element patch** ω_T is defined to be the union of the elements $K \in \mathcal{T}$ touching T, i.e. $T \cap K \neq \emptyset$.

Definition. A mesh is **shape regular** if for every element $T \in \mathcal{T}$ the ratio of the element diameter and the diameter of the largest ball that can be contained in T is uniformly bounded.

Shape regularity implies that there exist fixed constants c_1 and c_2 such that for any $T \in \mathcal{T}$ the following inequality holds:

$$c_1 h_{T_i} \leq h_T \leq c_2 h_{T_i} \ \forall \ T_i \in \omega_T. \tag{1.1}$$

Mesh generation or grid generation is the name given to the process of creating the computational domain where we seek the numerical solution of a given PDE. Depending on the domain that one wants to represent it can be a very complicated process. The main types of grids are: structured, unstructured or combinations of both. Adaptive finite element methods, like the ones we propose, generate unstructured meshes. For a more thorough discussion the interested reader is directed to [57].

1.1.1 Galerkin approximation

Let $\mathcal{L}$ denote a differential operator, let u be a function in some space S, and consider the PDE

$$\mathcal{L}u = f, \tag{1.2}$$

defined over a domain $\Omega \subset \mathbb{R}^n$. The weak form of (1.2) is find $u \in S$ such that

$$a(u, v) = f(v), \ \forall v \in V, \tag{1.3}$$

where V is a space of test functions, $a(\cdot, \cdot)$ is the bilinear form corresponding to $\mathcal{L}$ and $f(v)$ is a bounded linear functional. The finite element idea is to replace S and V, which are infinite dimensional spaces, with finite dimensional versions S_h and V_h. The spaces S_h and V_h are defined over the elements T of a mesh $\mathcal{T}$ of Γ. S_h is known as the space of trial functions and V_h is the space of **test functions**.

The corresponding discrete version of (1.3) is to find $u_h \in S_h$ such that

$$a(u_h, v_h) = f(v_h), \ \forall v_h \in V_h, \tag{1.4}$$

This is known as the **Galerkin method**. If S_h and V_h are equal we refer to it as a standard Galerkin method. Otherwise it is known as a **Petrov Galerkin Method**. We say that the approximation scheme is **conformal** if $S_h \subset S$ and $V_h \subset V$; otherwise it is said to be non-conformal. The space S_h is known as the **finite element space**.

Remarks:

(1) The spaces S and V are in general taken to be Banach spaces, i.e. complete normed vector spaces. In our application $S = V$ is a tangential Sobolev space defined in section 2.3. In particular S is taken to be the Hilbert space H^1.

(2) The bilinear form $a(\cdot, \cdot)$ is continuous on $S \times V$, hence it is bounded on $S \times V$.

(3) We chose to implement a standard Galerkin method i.e. $S = V$, $S_h = V_h$, such

that the true solution u of (1.8) satisfies

$$a(u, v) = f(v_h),\ \forall v_h \in V_h. \tag{1.5}$$

A Galerkin Approximation scheme satisfying (1.5) is said to be **consistent**. Equations (1.4) and (1.5) imply

$$a(u - u_h, v_h) = 0,\ \forall\ v_h \in S_h, \tag{1.6}$$

which is known as **Galerkin orthogonality**.

1.1.2 Finite Element

We use Ciarlet's definition of finite elements as triplets given in [15], section 2.3.

Definition. A **finite element** in $\mathbb{R}^n$ is a triplet (K, S_h, Σ) where:

(i) K is a closed subset of $\mathbb{R}^n$ with a non empty interior and Lipschitz-continuous boundary,

(ii) S_h is a space of real valued functions defined over the set K,

(iii) Σ is a finite set of linearly independent linear forms σ_i, $1 \leq i \leq N$, defined over the space S_h. It is assumed that Σ is S_h unisolvent in the following sense: Given any real scalars α_i, $1 \leq i \leq N$, there is a unique $p \in S_h$ which satisfies

$$\sigma_i(p) = \alpha_i,\ 1 \leq i \leq N.$$

It follows that there exist functions $\phi_i \in S_h$, $1 \leq i \leq N$, such that

$$\sigma_j(\phi_i) = \delta_{ij},\ 1 \leq j \leq N. \tag{1.7}$$

The functions ϕ_i form a basis for S_h, and the linear forms σ_i are called the degrees of freedom of the finite element. Equation (1.7) implies that one can regard $\{\sigma_i\}_{i=1}^N$ as the dual basis of $\{\phi_i\}_{i=1}^N$.

1.1.3 Implementation of a FEM

We now illustrate how these concepts apply to implement a FEM. Consider the Laplace equation with homogeneous Dirichlet boundary conditions:

$$\begin{aligned} -\triangle u &= f \text{ on } \Omega, \\ u &= 0 \text{ in } \partial\Omega. \end{aligned} \tag{1.8}$$

Here Ω denotes a domain in $\mathbb{R}^n$. The corresponding discrete bilinear form $a(\cdot, \cdot)$

and linear functional $f(v_h)$ of equation (1.4) are

$$\begin{aligned} a(u_h, v_h) &= \int_\Omega \nabla u_h \cdot \nabla v_h \; dx, \\ f(v_h) &= \int_\Omega f v_h \; dx, \end{aligned} \tag{1.9}$$

where dx denotes Lebesgue measure over Ω.

We chose to use a conformal standard Galerkin method. In the following discussion $\mathcal{T}$ to denotes a conforming shape regular mesh of Ω. The basis functions ϕ_i are taken to be continuous piecewise polynomials[1] with compact support. We use $z_i \in \Gamma_h$, $1 \leq i \leq N$ to represent the finite element nodal points, that is the set of points such that $\sigma_i(p) = p(z_i)$ for any $p \in S_h$. We construct ϕ_i such that $\phi_i(z_j) = \delta_{ij}$, $1 \leq i, j \leq N$ and $\phi_i|_T \equiv 0$ for $z_i \notin T$, $T \in \mathcal{T}$.

For example, suppose that S_h is taken to be the space of piecewise linear polynomials, let Ω be a domain in $\mathbb{R}^2$, let $T_\alpha \in \mathcal{T}$ be a triangular element with vertices $A(x_A, y_A)$, $B(x_B, y_B)$ and $C(x_C, y_C)$. Consider the affine transformation $\mathcal{A}(T_\alpha) : \mathbb{R}^2 \to T_\alpha$ such that

$$\begin{aligned} \mathcal{A}(0,0) &= A(x_A, y_A), \\ \mathcal{A}(1,0) &= B(x_B, y_B), \\ \mathcal{A}(0,1) &= C(x_C, y_C). \end{aligned} \tag{1.10}$$

Then the restrictions of the basis functions ϕ_A, ϕ_B and ϕ_C to the element T_α satisfy the equations

$$\begin{aligned} \mathcal{A}^{-1}(\phi_A|_{T_\alpha}) &= 1 - x - y, \\ \mathcal{A}^{-1}(\phi_B|_{T_\alpha}) &= x, \\ \mathcal{A}^{-1}(\phi_C|_{T_\alpha}) &= y. \end{aligned} \tag{1.11}$$

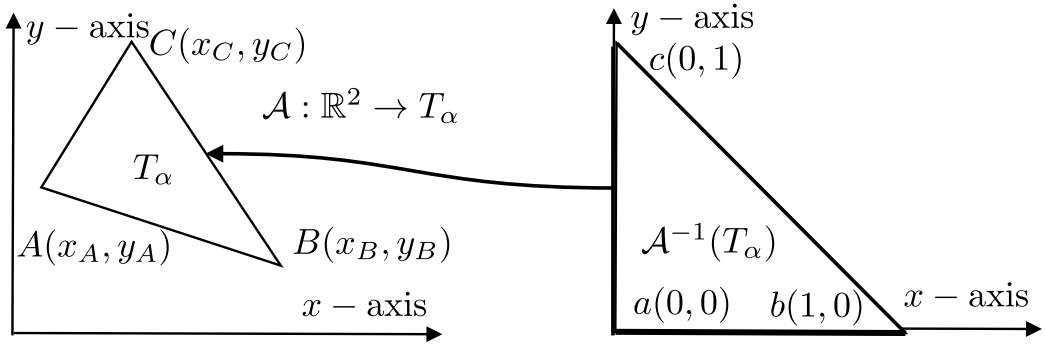

Figure 1-1: Affine transformation from an arbitrary element $T_\alpha \in \mathcal{T}$ to the reference element $\mathcal{A}(T_\alpha)$.

[1]Discontinuous piecewise polynomials are also used in the so called discontinuous Galerkin methods.

The ellipticity of $\triangle$ implies that $a(\cdot,\cdot)$ is coercive, that is,

$$a(\psi,\psi) \geq c_1\|\psi\|^2, \text{ for some } c_1 > 0 \text{ independent of } \psi. \tag{1.12}$$

Here we take ψ in some Hilbert space H, and $\|\cdot\|$ is the induced norm in H. Since $a(\cdot,\cdot)$ is a bounded coercive bilinear form on $S \times S$ it defines an inner product in S. The induced norm

$$|||v|||^2 = a(v,v), \tag{1.13}$$

is called the energy norm.

Because $u_h \in S_h$ it can be expressed as a linear combination of finite element basis functions

$$u_h = \sum_{i=1}^{N} \sigma_i(u_h)\phi_i. \tag{1.14}$$

Choosing $v_h = \phi_j$, $1 \leq j \leq N$, and defining $U_i \equiv u_h(z_i) = \sigma_i(u_h)$ we rewrite equation (1.4)

$$\sum_{i=1}^{N} U_i \left[\int_\Omega \nabla\phi_j \cdot \nabla\phi_i \, dx\right] = \int_\Omega f\phi_j \, dx, \; 1 \leq j \leq N, \tag{1.15}$$

which can be expressed in matrix form as

$$\begin{aligned} \mathbf{AU} &= \mathbf{F}, \\ [\mathbf{A}]_{i,j} &= \int_\Omega \nabla\phi_j \cdot \nabla\phi_i \, dx, \\ [\mathbf{U}]_i &= U_i, \\ [\mathbf{F}]_j &= \int_\Omega f\phi_j \, dx. \end{aligned} \tag{1.16}$$

The matrix $\mathbf{A}$ is the stiffness matrix and $\mathbf{F}$ is the load vector. It is clear from (1.9) that $\mathbf{A}$ is symmetric and by the construction of ϕ_i, $1 \leq i \leq N$, $\mathbf{A}$ is sparse. Furthermore because $\mathbf{A}$ is symmetric and $|||u_h|||^2 = a(u_h,u_h) = \mathbf{U}^T\mathbf{AU} > 0$ for $\mathbf{U} \neq 0$ it follows that $\mathbf{A}$ defined in (1.16) is symmetric positive definite.

Notice that (1.11) provides a way to construct the basis $\{\phi_j\}_j^N$ of S_h. In practice we do not need to explicitly compute the basis. We work with the functions defined on the reference triangle $\mathcal{A}(T_\alpha)$ (see Figure 1-1) and use a change of variable to calculate the stiffness matrix $\mathbf{A}$ and load vector $\mathbf{F}$ given by (1.16).

1.2 Error estimates

We find the numerical solution u_h by solving the linear system (1.16) and substituting the result into (1.14). A natural question is to ask how close u_h is to the true solution u. The quality of the numerical solution depends on the discretization parameters (mesh size) and the choice of the finite element space. We want the numerical solution

to converge to the true solution as the discretization parameter goes to zero. To guarantee convergence our numerical method should be consistent and stable. The selection of S_h is an important one as inadequate choices can lead to inconsistent schemes (cf. [4] Figure 1.2, [29] section 2.3.3). S_h must be chosen such that the approximation setting has the approximability property. We cite [29] Definition 2.1.4.

Definition. Let h be the discretization parameter, $S(h) \equiv S + S_h$ and let $\|\cdot\|_{S(h)}$ denote the norm of the space $S(h)$. Assume that

(a) $\|u_h\|_{S(h)} = \|u_h\|_{S_h}$ for all $u_h \in S_h$.

(b) S is continuously embedded in $S(h)$ i.e., $\|u\|_{S(h)} \leq c\|u\|_{S_h}$, $c > 0$.

The Galerkin approximation scheme is said to have the **approximability** property if

$$\lim_{h\to 0} \|u - u_h\|_{S(h)} = 0. \tag{1.17}$$

The approximation properties of S_h are often derived using the Bramble-Hilbert Lemma [9], [10] or similar of arguments.

1.2.1 A priori and a posteriori error estimates

There are two basic types of error estimates, a priori and a posteriori. **A priori** error estimates are error bounds that use information about the unknown solution u to estimate the error before we compute the approximate solution u_h. **A posteriori** error estimates are computable estimates that use information gathered from the problem data and numerical solution. In sections 3.2 and 3.3 we prove L^2 and pointwise error estimates that are used to implement an adaptive finite element method.

Inequalities (1.18) through (1.23) show "standard" a priori and a posteriori error estimates, for domains in $\mathbb{R}^n$. In these estimates u is the solution to the variational problem (1.3), $u \in V \cap H^{k+1}(\Omega)$, $u_h \in S_h$ is the solution of (1.4), while h represents the mesh size.

Energy norm a priori estimate: (cf. (58) Chapter 4 of [54].)

$$|||u - u_h|||_{(\Omega)} \leq Ch^k |u|_{H^{k+1}}(\Omega), \text{ for some } k \in (0, 1]. \tag{1.18}$$

L^2 a priori estimate: (cf. (60) Chapter 4 of [54].)

$$\|u - u_h\|_{L^2(\Omega)} \leq Ch^{2k} |u|_{H^{k+1}(\Omega)}, \text{ for some } k \in (0, 1]. \tag{1.19}$$

L^∞ a priori estimate:

$$\|u - u_h\|_{L^\infty(\Omega)} \leq C \log\left(\frac{1}{h}\right) h^{k+1} |u|_{W^{k+1}_\infty(\Omega)}, \text{ for } 0 \leq k \leq \deg(S_h). \tag{1.20}$$

Energy norm a posteriori estimate:

$$|||u - u_h|||^2 \leq C \sum_{T\in\mathcal{T}} \left\{ h_T^2 \|f + \triangle u_h\|^2_{L^2(\Omega)} + h_T \|[\![\nabla u_h]\!]\|^2_{L^2(\partial\Omega)} \right\}. \tag{1.21}$$

L^2 a posteriori error estimate:

$$\|u - u_h\|_{L^2(\Omega)} \leq C \sum_{T \in \mathcal{T}} \left\{ h_T^4 \|f - u_h\|^2_{L^2(\Omega)} + h_T^3 \|[\![\nabla u_h]\!]\|^2_{L^2(\partial T)} \right\}. \tag{1.22}$$

L^∞ a posteriori error estimate: Let $\underline{h} = \min_{T \in \mathcal{T}} \{h_T\}$, then for all $x \in \Omega$ the following bound holds

$$|u - u_h|(x) \leq C(1 + \ln \underline{h}) \max_{T \in \mathcal{T}} \{ h_T^2 \|f + \triangle u_h\|_{L^\infty(T)} + h_T \|\nabla u_h\|_{L^\infty(\partial T)} \}. \tag{1.23}$$

1.2.2 Adaptive finite element method

Given a mesh and finite element space S_h there are two main ways that one can choose to reduce the finite element error. The first one is to change the mesh. This is typically done through a refinement process. The second way is to exchange S_h for a space with better approximation properties. For example, one can use higher degree polynomials as the basis elements of S_h while maintaining a fixed mesh.

Adaptive finite element methods (AFEMs) use a posteriori error estimates to direct the computational effort to the regions of the mesh where the error is bigger. They contrast with **uniform refinement** where the error is reduced by refining the mesh uniformly. A classic adaptive finite element method repeats the scheme SOLVE $\rightarrow$ ESTIMATE $\rightarrow$ MARK $\rightarrow$ REFINE (cf. [46]) until the a posteriori error estimate is less than a threshold. AFEMs are more efficient than uniform refinement when solving problems with singularities or other strong local variations of the solution. If we reduce the error through mesh refinement we call the method h-adaptive. If instead we increase the polynomial degree we say that we have a p-adaptive method. In practice a combination of h and p adaptivity can be implemented.

A good adaptive algorithm equi-distributes the error over the computational mesh. It uses less degrees of freedom (computational nodes) to produce a solution with a given accuracy than a uniform refinement algorithm. An important practical question is how to decide between uniform and adaptive refinement. The answer depends on the problem in question, the convergence rates and the number of floating point operations per step required for each scheme. If the solution and domain are smooth enough then uniform refinement is recommended. If we want high-accuracy and the solution presents strong localized variations then adaptivity may be a good option. One advantage of adaptive over uniform refinement, is that the first requires less degrees of freedom to achieve a given accuracy.

1.3 Surface Finite element method

In this section we discuss the main differences between a finite element method for domains in $\mathbb{R}^n$ and a Surface Finite Element Method (SFEM). We use Γ to denote an

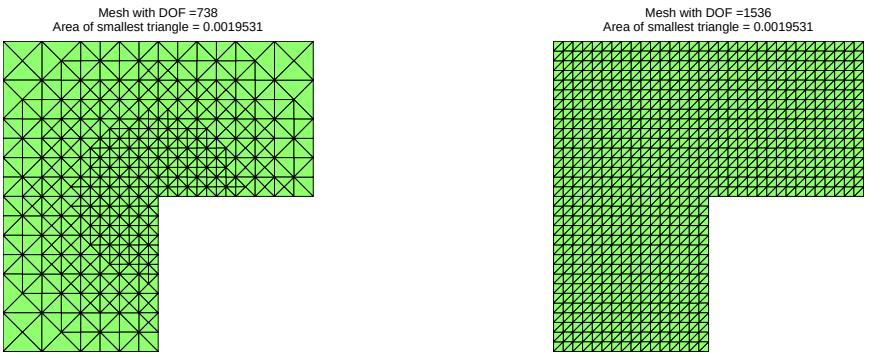

Figure 1-2: Left figure shows a mesh obtained using adaptive refinement, the right figure shows a mesh obtained using uniform refinement.

$n-1$ dimensional surface embedded in $\mathbb{R}^n$ and consider the elliptic model equation:

$$\begin{aligned} -\triangle_\Gamma u &= f \text{ on } \Gamma, \\ u &= 0 \text{ in } \partial\Gamma, \text{ or} \\ \partial\Gamma &= \emptyset. \end{aligned} \tag{1.24}$$

If $\partial\Gamma = \emptyset$, then (1.24) does not have a unique solution. In that case to guarantee uniqueness we require the solution to satisfy $\int_\Gamma u \ \mathrm{d}\sigma = 0$. Existence is ensured by requiring $\int_\Gamma f \ \mathrm{d}\sigma = 0$. The operator $\triangle_\Gamma$ is known as the Laplace-Beltrami operator. It is the manifold equivalent of the Laplace operator. One interesting property of the Laplace-Beltrami operator is that, up to a sign, its eigenvalues and eigenfunctions are invariant to isometric transformations of Γ. This is one of the reasons why the eigenvalues of the Laplace-Beltrami operator are used in diffusion geometry as an isometric invariant descriptor of Γ (cf. [2], [61], [52]). A more detailed explanation of the Laplace-Beltrami operator is given in section 2.2.

In order to compute the numerical solution, we replace Γ by a polyhedral approximation Γ_h of it. The faces of Γ_h are assumed to be simplices. Another possible choice that could be the object of future work is the use of curved meshes [49].

We consider an initial conforming shape regular mesh with nodes lying in Γ; and assume that all the refined meshes $\mathcal{T}_h$ have all their nodes lying in Γ and are also shape regular. Typical refinement algorithms in $\mathbb{R}^n$ preserve shape regularity. This also seems to be the case over surfaces, but we are unaware of a proof (c.f. [20] Section 2.2).

We define a discrete version of (1.9) over the discrete surface Γ_h:

$$\begin{aligned} a_h(u_h, v_h) &= \int_{\Gamma_h} \nabla_{\Gamma_h} u_h \cdot \nabla_{\Gamma_h} v_h \ \mathrm{d}\sigma_h, \\ f(v_h) &= \int_{\Gamma_h} f_h v_h \ \mathrm{d}\sigma_h, \end{aligned} \tag{1.25}$$

where ∇_{Γ_h} is the tangential gradient over Γ_h, $\mathrm{d}\sigma_h$ denotes Lebesgue measure over

Γ_h and f_h is an approximation of f defined on Γ_h. A precise definition of ∇_{Γ_h} is given in section 2.2.

Equations (1.10) and (1.11) still hold with the difference that now we need three coordinates to describe the vertices of T. That is, $A = A(x_A, y_A, z_A)$, $B = B(x_B, y_B, z_B)$ and $C = C(x_C, y_C, z_C)$; cf. Figure 1-3.

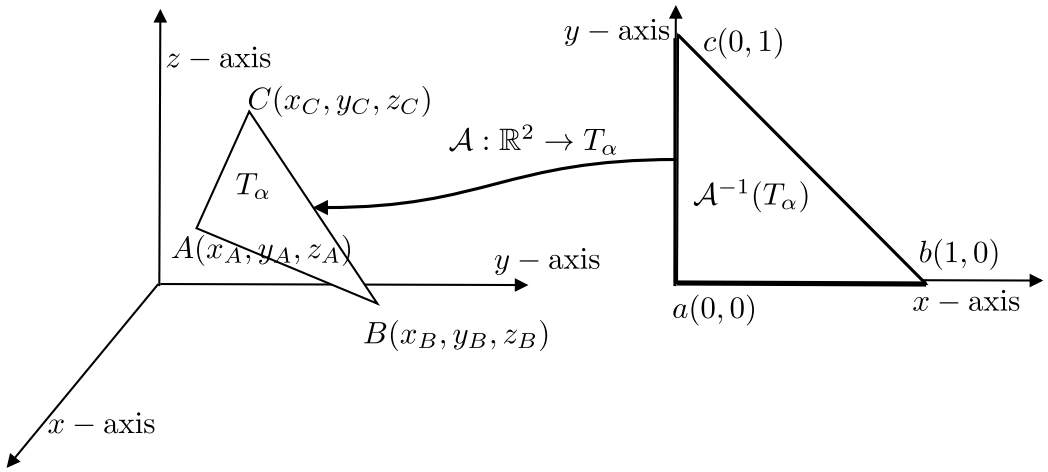

Figure 1-3: Affine transformation to an arbitrary element $T_\alpha \in \mathcal{T}$ from the reference element $\mathcal{A}(T_\alpha)$.

Equations (1.5), (1.15) and (1.16) change to

$$a_h(u^\ell, v_h) = f_h(v_h), \ \forall v_h \in V_h, \tag{1.26}$$

$$\sum_{i=1}^{N} U_i \left[\int_{\Gamma_h} \nabla_{\Gamma_h}\phi_j \cdot \nabla_{\Gamma_h}\phi_i \ \mathrm{d}\sigma_h \right] = \int_{\Gamma_h} f_h\phi_j \ \mathrm{d}\sigma_h, \ 1 \le j \le N, \tag{1.27}$$

and

$$\begin{aligned} \mathbf{AU} &= \mathbf{F_h}, \\ [\mathbf{A}]_{i,j} &= \int_{\Gamma_h} \nabla_{\Gamma_h}\phi_j \cdot \nabla_{\Gamma_h}\phi_i \ \mathrm{d}\sigma_h, \\ [\mathbf{U}]_i &= U_i, \\ [\mathbf{F_h}]_j &= \int_{\Omega} f_h\phi_j \ \mathrm{d}\sigma_h. \end{aligned} \tag{1.28}$$

The term u^ℓ in (1.26) is a lift of u to Γ_h defined in Section 2.2.1.

1.4 Adaptive Surface Finite Element (ASFEM)

Some interesting applications where it is necessary to solve surface PDEs include applications to Materials Science, Thin Films, Fluid Interfaces and Image Processing; cf. [16, 33, 34, 48, 51] among others. Previous work for ASFEM includes residual

a posteriori error estimates in the energy norm for SFEMs [20] and some variations such as [36, 60, 42, 23, 8].

A posteriori errors for controlling the energy norm (1.13) are discussed in [24] and [20]. Typical error estimates for surfaces have a residual component (Galerkin error) and a geometric component. Inequalities (1.21) through (1.23) are examples of residual estimates.

The geometric component arises because our polyhedral approximation $\Gamma_h \neq \Gamma$. This is known as a variational crime [55]. The variational crime decreases as $\Gamma_h \to \Gamma$. For the energy case the geometric component of the a posteriori estimate is of higher order and the estimate is asymptotically dominated by the residual. It was proved in [20] that for properly defined approximations f_h of f the following bound holds:

$$\|\nabla_\Gamma(u-u_h)\|_{L^2(\Gamma)} \leq C\left(\sum_{T\in\mathcal{T}} \mathbf{B}(\omega_T)\eta_1(T)^2\right)^{1/2} + C\|(\mathbf{P}-A_h^\ell)\mathbf{M}\nabla_\Gamma u_h^\ell\|_{L^2(\Gamma)}. \quad (1.29)$$

Here $\mathbf{B}(\omega_T)$ is a multiplicative geometric term satisfying $\mathbf{B}(\omega_T) \to 1$ as the mesh size goes to zero, η_1 is a standard energy residual error indicator (Galerkin error), ω_T is the patch of elements $K \in \mathcal{T}$ touching the element T, and $\|(\mathbf{P}-A_h^\ell)\mathbf{M}\nabla_\Gamma u_h^\ell\|_{L^2(\Gamma)}$ is a geometric additive term. The residual term $\left(\sum_{T\in\mathcal{T}} \mathbf{B}(\omega_T)\eta_1(T)^2\right)^{1/2}$ is of linear order with respect to the mesh size while the geometric term $\|(\mathbf{P}-A_h^\ell)\mathbf{M}\nabla_\Gamma u_h^\ell\|_{L^2(\Gamma)}$ depends quadratically on the mesh size.

A priori error estimates, for S_h consisting of piecewise linear polynomials defined over a polyhedral Γ_h, also suggest that the error measured in the energy norm should decrease linearly with respect to the mesh size. This assertion is illustrated by the following a priori bounds (cf. page 2 of [19], [24]).

$$\|\nabla_\Gamma(u-u_h)\|_{L^2(\Gamma)} \leq Ch\|u\|_{H^2(\Gamma)} + Ch^2\|u\|_{H^1(\Gamma)}. \quad (1.30)$$

$$\|u-u_h\|_{L^2(\Gamma)} \leq Ch^2\|u\|_{H^2(\Gamma)}. \quad (1.31)$$

In sections 3.2 and 3.3 we present efficient a posteriori L^2 and pointwise error estimates for elliptic equations on surfaces. In contrast with the energy norm estimate (1.29) the geometric and residual components are of the same order. Thus adaptivity can be driven by the geometric error in fine meshes as illustrated in Figure 3-1. A byproduct of our analysis is a more local version of the Bramble-Hilbert Lemma (see Section 2.4.3). In Section 4.3 we extend our results to parabolic PDEs using the elliptic reconstruction technique proposed in [41].

Chapter 2

Technical Preliminaries

In this section we introduce the notation, and geometric definitions that will be used in the subsequent chapters. We briefly state the basic definition of a Sobolev space and extend it to define tangential Sobolev spaces. In Section 2.4 we introduce the Scott-Zhang interpolant; and then we proceed to discuss its approximation properties.

2.1 Surface geometry and notation

We recall that Γ is used to denote an $(n-1)$-dimensional smooth oriented surface embedded in $\mathbb{R}^n$, and Γ_h is a polyhedral approximation of Γ. We assume that Γ_h has simplicial faces denoted by T. This assumption helps in obtaining "cleaner" proofs. In practice the faces need not to be simplices. For example, in 2-D, other popular choices are rectangular faces or mixes of different shapes.

We assume that the number of elements in the patch ω_T is bounded by a fixed constant for any $T \in \mathcal{T}$. This is always true for shape regular meshes over $\mathbb{R}^n$, but does not necessarily hold for arbitrary surface meshes. However if the number of elements in each ω_T is bounded in the initial mesh, standard adaptive refinement algorithms maintain the bound for subsequent meshes ([20] section 2.2).

The signed distance function from a point x to Γ is denoted by $d(x)$. The outward unit normal vectors to Γ and Γ_h are denoted by $\vec{\nu}(x)$ and $\vec{\nu}_h(x)$ respectively. We let $\vec{s}_1(T)$, $\vec{s}_2(T)$ and $\vec{s}_3(T)$ be vectors aligned with the sides of T such that the chain $\vec{s}_1(T) \to \vec{s}_2(T) \to \vec{s}_3(T)$ traverses the boundary ∂T of T with positive orientation. Then $\vec{\nu}(x)$ and $\vec{\nu}_h(x)$ can be computed with the following equations:

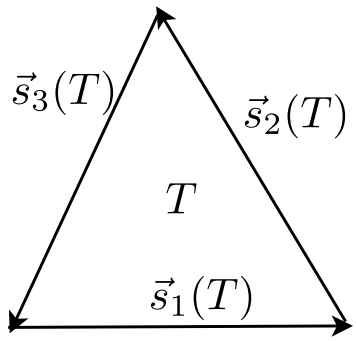

Figure 2-1: Positively oriented boundary ∂T

$$\vec{\nu}(x) = \nabla d(x), \tag{2.1}$$

and

$$\vec{\nu}_h(x) = \frac{\vec{s}_1 \times \vec{s}_2}{\|\vec{s}_1 \times \vec{s}_2\|}. \tag{2.2}$$

The Hessian $\mathbf{H}(x) := D^2 d(x)$ of $d(x)$ is also called the Weingarten map. Its nonzero eigenvalues are the principal curvatures of Γ. Since $|\vec{\nu}(x)| = 1$, $\vec{\nu}^T \mathbf{H} = \vec{0}^T$ and $\mathbf{H}\vec{\nu} = \vec{0}$.

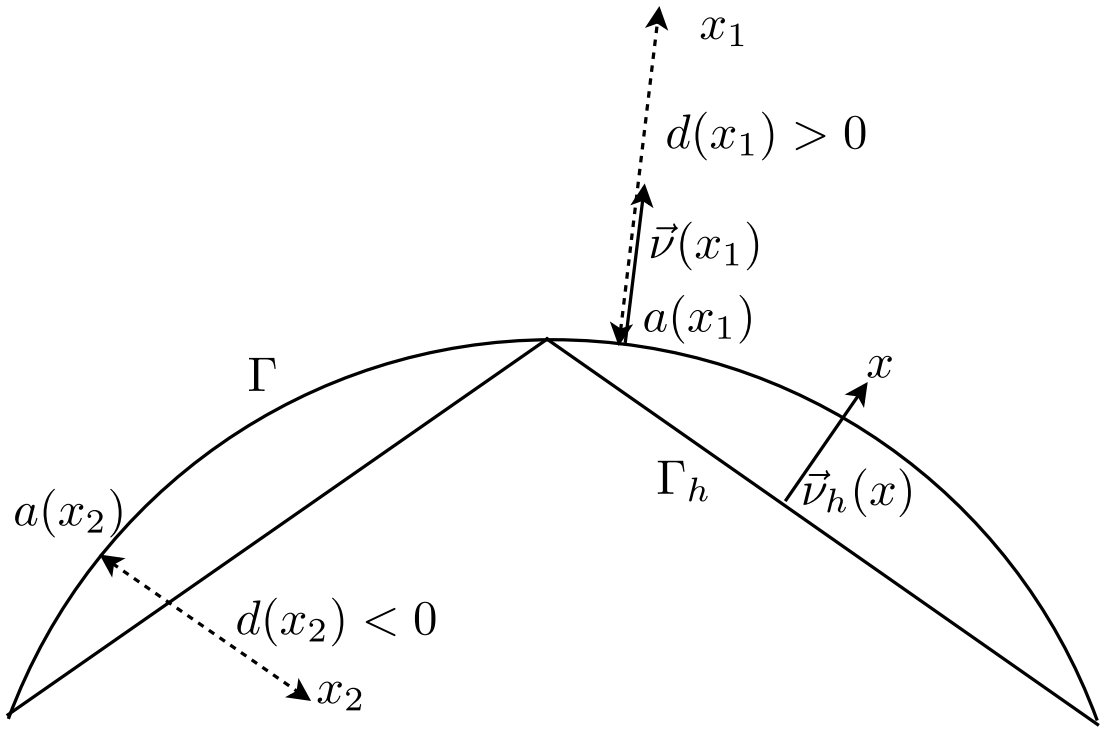

Figure 2-2: Surface and polyhedral approximation

Definition. The **projection** of a point $x \in \mathbb{R}^3$ is defined by the equation

$$a(x) : U \to \Gamma \; a(x) = x - d(x)\vec{\nu}(x) \quad \text{for } x \in U, \tag{2.3}$$

If Γ is smooth enough there is a tubular region U containing Γ where the restriction of (2.3) to U is unique [32].

Throughout this document we assume that Γ and Γ_h are such that $a : \Gamma_h \to \Gamma$ is a bijection. For shape regular meshes, and $d(x)$ small enough the following bound holds

$$\|d\|_{L^\infty(T)} + h_T \|\vec{\nu} - \vec{\nu}_h\|_{L^\infty(T)} \lesssim h_T^2, \; \forall T \in \mathcal{T}. \tag{2.4}$$

By $a \lesssim b$ we mean $a \leq Cb$, where C depends on global properties of Γ but not other essential quantities. Let $\mu_h(x)$ be the Jacobian of the transformation $a(x)|_{\Gamma_h} : \Gamma_h \to \Gamma$, so that

$$\mu_h d\sigma_h = d\sigma. \tag{2.5}$$

Definition. (See [30] appendix C.1.) Let $\Omega \subset \mathbb{R}^n$ be open and bounded, $k \in \{1, 2, \ldots\}$. We say that $\partial\Omega$ is C^k if for each point $x^0 \in \partial\Omega$ there exist $r > 0$ and a C^k

function $\gamma : \mathbb{R}^{n-1} \to \mathbb{R}$ such that upon relabelling and reorienting axes if necessary we have

$$\Omega \bigcap B(x^0, r) = \{x \in B(x^0, r) : x_n > \gamma(x_1, \ldots, x_{n-1})\}.$$

Here $B(x^0, r)$ denotes the n-dimensional ball of radius r centered at the point x^0.

2.1.1 Projection matrices

The projection matrices onto the tangent spaces of Γ and Γ_h are denoted by $\mathbf{P}(x)$ and $\mathbf{P}_h(x)$ respectively. The matrices can be computed using the following expressions:

$$\mathbf{P}(x) = \mathbf{I} - \vec{\nu} \otimes \vec{\nu}, \qquad \mathbf{P}_h(x) = \mathbf{I} - \vec{\nu}_h \otimes \vec{\nu}_h. \tag{2.6}$$

Here $\otimes$ is used to denote the vector tensor product defined by the equation

$$[\vec{a} \otimes \vec{b}]_{i,j} = a_i b_j.$$

2.2 Surface Derivatives.

Definition. Let $\xi(x)$ be a function defined on a tubular region U of Γ. The surface or **tangential gradient** of $\xi(x)$ is given by (see e.g. [26])

$$\nabla_\Gamma \xi(x) = \nabla \xi(x) - \nabla \xi(x) \cdot \vec{\nu}(x) \vec{\nu}(x) = [\underline{D}_1 \xi(x), \ldots, \underline{D}_n \xi(x)]. \tag{2.7}$$

Here $\underline{D}_i = \frac{\partial}{\partial x_i}() - \nu_i \sum_{j=1}^n \frac{\partial}{\partial x_j}() \nu_j$.

Definition. The **Laplace-Beltrami** operator is defined as the tangential divergence of the tangential gradient, that is

$$\triangle_\Gamma \xi(x) = \nabla_\Gamma \cdot \nabla_\Gamma \xi(x) = \sum_{i=1}^n \underline{D}_i \underline{D}_i \xi(x). \tag{2.8}$$

An equivalent way of writing (2.8), suitable for numerical computation, is

$$\triangle_\Gamma \xi(x) = \mathrm{tr}(D^2 u) + \vec{\nu}[D^2 u]\vec{\nu}^T - \mathrm{tr}(\mathbf{H})\vec{\nu} \cdot \nabla u. \tag{2.9}$$

For more details see [20] and [27].

2.2.1 Lifts and extensions

See [24, 20] for more details. We extend v defined on Γ to U by

$$v^\ell(x) = v(a(x)), \ x \in U. \tag{2.10}$$

For v_h defined on Γ_h we define the lift $\tilde{v}_h$ by $v_h(x) = \tilde{v}_h(a(x))$, where $a(x) \in \Gamma$ is as in (2.3). For v_h defined on Γ_h and $x \in U$ we extend $\tilde{v}_h$ to U by the equation

$v_h^\ell(x) = \tilde{v}_h(a(x))$. The relationship between $\nabla_\Gamma u_h^\ell(a(x))$ and $\nabla_{\Gamma_h} u_h(x)$ is given by

$$\nabla_\Gamma u_h^\ell(a(x)) = [(\mathbf{I} - d\mathbf{H})(x)]^{-1} \left[\mathbf{I} - \frac{\vec{\nu}_h \otimes \vec{\nu}}{\vec{\nu}_h \cdot \vec{\nu}}\right] \nabla_{\Gamma_h} u_h(x). \tag{2.11}$$

Definition. Following [20] we define the **energy inner product transformation** $\mathbf{A}_h$:

$$\mathbf{A}_h(x) = \mathbf{A}_h^\ell(a(x)) = \frac{1}{\mu_h(x)}[\mathbf{P}(x)][(\mathbf{I} - d\mathbf{H})(x)][\mathbf{P}_h(x)][(\mathbf{I} - d\mathbf{H})(x)][\mathbf{P}(x)]. \tag{2.12}$$

Equation 2.22 of [20] yields

$$\int_{\Gamma_h} \nabla_{\Gamma_h} v_h \cdot \nabla_{\Gamma_h} \psi_h \ \mathrm{d}\sigma_h = \int_\Gamma [\nabla_\Gamma v_h^\ell(a(x))]^T [\mathbf{A}_h^\ell][\nabla_\Gamma \psi_h^\ell(a(x))] \ \mathrm{d}\sigma. \tag{2.13}$$

2.3 Function spaces

Let Ω be a domain in $\mathbb{R}^n$.

Definition. The following definitions are standard, the reader is referred to Chapters 1 and 2 of [11] for additional details. For $1 \leq p < \infty$, let

$$\|f\|_{L^p(\Omega)} := \left(\int_\Omega |f(x)|^p \ dx\right)^{1/p}, \tag{2.14}$$

and for $p = \infty$

$$\|f\|_{L^\infty(\Omega)} := \text{ess sup}\{|f(x)| : x \in \Omega\}. \tag{2.15}$$

Let $1 \leq p \leq \infty$ the **Lebesgue space** $L^p(\Omega)$ is defined as

$$L^p(\Omega) := \{f : \|f\|_{L^p(\Omega)} < \infty\}. \tag{2.16}$$

Definition. The **Sobolev space** $W_p^k(\Omega)$ is defined as

$$W_p^k(\Omega) := \{f \in L^p(\Omega) : D^\alpha f \in L^p(\Omega), \ |\alpha| \leq k\}, \tag{2.17}$$

here D^α denotes a weak derivative, and α is a multi-index.

Definition. The Sobolev space $W_2^k(\Omega)$ is referred as the **Hilbert space** $H^k(\Omega)$.

In a similar way we can define the **tangential Sobolev space**$W_p^k(\Gamma)$ and **tangential Hilbert space** $H^k(\Gamma)$ by substituting the weak derivatives D^α in (2.17) by tangential weak derivatives $\underline{D}^\alpha$ as defined in equation (2.7) (cf. Section 4.2 of [8]).

2.4 Interpolants and approximation results

Interpolation is used to carry out error analysis for FEM. For example in Section 3.2 we use interpolation to find a bound for the expression

$$a(u - u_h^\ell, v) = \int_\Gamma \nabla_\Gamma (u - u_h^\ell) \cdot \nabla_\Gamma v \ \mathrm{d}\sigma.$$

Using equation (3.5) of [20] we end with an expression containing factors of the form $(v^\ell - v_h)$ defined over Γ_h. The term $v_h \in S_h$ is taken to be an interpolant of $v^\ell \notin S_h$. The accuracy of the error estimate will depend on the approximation properties of the interpolant used. A powerful tool used to prove approximation properties of such interpolants is the Bramble-Hilbert Lemma. We cite [11] Lemma (4.3.8).

Lemma 2.4.1 ***(Bramble-Hilbert)*** *Let B be a ball in Ω such that Ω is star-shaped with respect to B and such that its radius $\rho > \frac{1}{2}\rho_{max}$. Let $Q^m u$ be the Taylor polynomial of degree m of u averaged over B where $u \in W_p^{m+1}(\Omega)$ and $p \geq 1$. Then*

$$|u - Q^m u|_{W_p^k(\Omega)} \leq C_{m,n} h^{m-k} |u|_{W_p^m(\Omega)}, \ k = 0, 1, \ldots m, \tag{2.18}$$

where $h = diam(\Omega)$.

Common interpolation schemes for smooth functions are Hermitian and Lagrangian. The results obtained in Section 3.2 can be proved using Lagrange interpolation ([11] Definition (3.3.1)). However the proof of the pointwise a posteriori estimate uses Green's functions. Lagrange interpolation requires us to be able to sample point values to approximate the function. Since Greens functions have local singularities we can not use Lagrange interpolation to prove our pointwise estimates. Thus we pick an interpolant suitable for non-smooth functions. Some examples of such interpolants are Clément and Scott-Zhang. We chose a Scott-Zhang type interpolant because, in contrast to Clément schemes, it is a projection.

In [20] the authors defined and proved approximation properties for a Lagrange interpolant on Γ_h, but their operator only yields the first-order approximation properties needed for energy estimates. Such estimates are simpler because $u \in W_p^1(\Gamma)$ implies $u^\ell \in W_p^1(\Gamma_h)$. We must instead consider broken spaces, since $u \in W_p^2(\Gamma)$ implies only $u^\ell \in W_p^2(T)$ for $T \in \mathcal{T}$. Typical proofs of higher-order approximation properties for Scott-Zhang type interpolants employ a Bramble-Hilbert lemma which in our context would require $u^\ell \in W_p^2(\omega_T)$ for *patches* ω_T, so the standard proof does not apply. The main technical ideas in this section are essentially contained in Theorem 3.1 of [58], though they are applied there in a somewhat different context.

2.4.1 Interpolant (Scott-Zhang)

Let $\mathcal{T}$ and T be as defined previously, let eT_z be a face of the simplex T, and let $\mathcal{N} := \{\text{Finite element nodes}\}$. For all nodes $z \in \mathcal{N}$ define:

$$F_z := \begin{cases} T, \text{ if } z \text{ is an interior node of } T, \\ eT_z, \text{ if } z \text{ is an interior point of } eT_z, \\ eT_z \text{ for an arbitrary } eT_z \ni z, \text{ if } z \text{ is contained in more than} \\ \text{ one face.} \end{cases} \tag{2.19}$$

Let $\{\varphi_z\}_{z\in\mathcal{N}}$ be the nodal basis for S_h, i.e., $\varphi_{z_j}(z_j) = \delta_{ij}$ and $\deg(\varphi_z) = n$. Let $\{\psi_z\}_{z\in\mathcal{N}}$ be the basis dual to $\{\varphi_z\}_{z\in\mathcal{N}}$, i.e. $\int_{F_z} \psi_{zi}\varphi_{zj} = \delta_{ij}$, where z_i, z_j are nodes associated with the simplex F_z and $\psi_z : \mathcal{P}_n^{d-1} \to \mathbb{R}$ is a polynomial of degree n.

Following [53], we define the interpolant $I_h v^\ell$ of v^ℓ as

$$I_h v^\ell = \sum_{z\in\mathcal{N}} \varphi_z \int_{F_z} \psi_z(\zeta) v^\ell(\zeta)\, d\zeta. \tag{2.20}$$

I_h is a projection, that is, $I_h s = s \ \forall s \in S_h$.

Lemma 2.4.2 *For any node $z \in \mathcal{N}$*

$$\|\psi_z\|_{L^q(F_z)} \lesssim h_T^{-\dim(F_z)(1-1/q)}. \tag{2.21}$$

Proof To prove (2.21) let $A : \hat{F}_z \to F_z$ be an affine transformation as described in [53] equation (3.1):

$$A(\hat{x}) = B\hat{x} + x_0.$$

From [53] equation (3.3) it follows that

$$\|\hat{\psi}_j\|_{L^q(\hat{F}_z)} = \left(\int_{\hat{F}_z} |\det(B)\psi_j(A(\hat{x}))|^q \, d\hat{x} \right)^{1/q}.$$

After changing variables we get

$$\|\hat{\psi}_j\|_{L^q(\hat{F}_z)} = \left(\int_{F_z} |\det(B)\psi_j(x)|^q \frac{1}{\det(B)} \, dx \right)^{1/q} = \det(B)^{1-1/q} \|\psi\|_{L^q(F_z)}.$$

The result then follows since $\det(B) \lesssim h_T^{\dim(F_z)}$ [53] equation (3.2).

Lemma 2.4.3 *Let $\dim\{T\} = d$, $0 < h_T < 1$. Since $|\varphi_z| \le 1$, it follows that*

$$\|\varphi_z\|_{W_p^k(T)} \lesssim h_T^{-k+d/p}. \tag{2.22}$$

Proof To verify (2.22) we consider the change of variable $x = h\hat{x}$ and define $\hat{\varphi}_z(\hat{x}) := \varphi_z(h\hat{x})$ then,

$$\|\hat{\varphi}_z\|_{W_p^k(\hat{T})} = \sum_{t=0}^{k} \|D^t \hat{\varphi}_z\|_{L^p(\hat{T})}.$$

Each term $\|D^t\hat{\varphi}_z\|_{L^p(\hat{T})} = h_T^{t-d/p}\|D^t\varphi_z\|_{L^p(T)}$ (c.f [45] section 1.2). Because $\|\hat{\varphi}_z\|_{W_p^k(\hat{T})}$ is bounded and $0 < h < 1$, it follows that $h^{k-d/p} \leq h^{t-d/p}$ for all $t = 0, 1, \ldots, k$, thus

$$h_T^{k-d/p}\|\varphi_z\|_{W_p^k(T)} \leq \|\hat{\varphi}_z\|_{W_p^k(\hat{T})},$$
$$\|\varphi_z\|_{W_p^k(T)} \leq h_T^{-k+d/p}$$

concluding the verification of inequality (2.22).

Remark From this point on we let I_h denote the Scott-Zhang interpolant defined on (2.20). We consider finite element spaces S_h of arbitrary degree n over meshes $\mathcal{T}$ of arbitrary space dimension, since the proof is no more difficult and more general results are of interest when considering SFEM in higher space dimensions; cf. [19].

2.4.2 Trace inequality

For any element $T \in \mathcal{T}$ and $\Phi \in W_p^1(T)$, $1 \leq p < \infty$, a standard scaled trace inequality (cf. [11] Theorem 1.6.6) yields

$$\|\Phi\|_{L^p(\partial T)} \lesssim h_T^{-1/p}\|\Phi\|_{L^p(T)} + h_T^{1-1/p}\|\nabla\Phi\|_{L^p(T)}. \tag{2.23}$$

2.4.3 Approximation properties

If p and ℓ satisfy $1 \leq p \leq \infty$ and $\ell \geq 1$ if $p = 1$, and $\ell > \frac{1}{p}$ otherwise, then equation 4.3 of [53] and Lemma 1.130 of [29] give approximation properties for the Scott-Zhang interpolator of the form

$$\|I_h\Phi - \Phi\|_{W_p^m(T)} \lesssim h_T^{\ell-m}|\Phi|_{W_p^\ell(\omega_T)}.$$

For our purpose we consider functions Φ that lie in $W_p^\ell(K)$ for all $K \in \omega_T$ but that may not be in $W_p^\ell(\omega_T)$. Assuming $\Phi \in W_1^1(\omega_T)$ in order to guarantee continuity of traces, our goal is to prove that

$$\|I_h\Phi - \Phi\|_{W_p^m(T)} \lesssim h_T^{\ell-m} \sum_{K\in\omega_T} |\Phi|_{W_p^\ell(K)}.$$

Lemma 2.4.4 and Theorem 2.4.5 below were inspired by [58].

Lemma 2.4.4 *Let $z \in \mathcal{N}$ and let F_z be a simplex of dimension $d-1$ defined as in (2.19) and let $T \in \mathcal{T}$ be a simplex of dimension d such that $z \in T \cap F_z$. Define ω_T to be the set of all simplices in $\mathcal{T}$ that touch T. For $p \geq 1$ let $\Phi \in W_p^\ell(\tilde{T})$ for some $1 \leq \ell \leq n+1$ and for all $\tilde{T} \in \mathcal{T}$. Let $p_T \in S_h$ be the $\ell-1$-st degree average Taylor polynomial of Φ over the simplex T, as defined in Lemma 4.3.8 of [11]. Pick q such that $\dfrac{1}{p} + \dfrac{1}{q} = 1$ and assume that $\mathcal{T}$ is a shape regular conforming mesh. Then for*

$\Phi \in W_1^1(\omega_{\tilde{T}})$

$$\left| \int_{F_z} \psi_z(\Phi - p_T) \, ds \right| \lesssim h_T^{-(d-1)(1-1/q)+(\ell-1/p)} \sum_{\tilde{T} \in \omega_T} |\Phi|_{W_p^\ell(\tilde{T})}. \tag{2.24}$$

Proof Observe that if $T = F_z$ the result follows directly from the Bramble-Hilbert Lemma (2.18). If $T \cap F_z$ is a face of T then the claim follows from the Trace Inequality (2.23) and Bramble-Hilbert Lemma. Hence assume that $T \cap F_z$ is a simplex of dimension at most $d-2$, and let $\{T_j\}_{j=1}^M$ be a chain of d-dimensional simplices inside of ω_T such that $T_{j+1} \cap T_j = F_j$ are $(d-1)$-dimensional simplices, $z \in F_j$ for $1 \leq j \leq M$, $T_1 = T$ and F_z is a face of T_M but $F_z \neq F_{M-1}$. M is uniformly bounded over $\mathcal{T}$, by our assumptions. (2.20) yields

$$\int_{F_z} \psi_z(\Phi - p_T) \, ds = I_h(\Phi - p_T)(z).$$

Let ψ_j be the dual to φ_z on F_j as in (2.20) so that $\int_{F_j} \psi_j \varphi_z = 1$ and $\int_{F_j} \psi_j v_h = v_h(z)$, $v_h \in S_h$. Note that in general $\psi_z \neq \psi_j$ since $F_z \neq F_j$. Then $(p_{T_{j+1}} - p_{T_j})(z) = \int_{F_j} \psi_{T_j}(p_{T_{j+1}} - p_{T_j}) \, d\sigma$, so that using a telescoping sum along with Hölders and triangle inequalities we obtain

$$\begin{aligned} \int_{F_z} \psi_z(\Phi - p_T) \, ds = & \int_{F_z} \psi_z(\Phi - p_{T_M}) \, ds + \sum_{j=1}^{M-1} \int_{F_j} \psi_{\alpha_j}(p_{T_{j+1}} - p_{T_j}) \, ds \\ \leq & \|\psi_z\|_{L^q(F_z)} \|\Phi - p_{T_M}\|_{L^p(F_z)} \\ & + \sum_{j=1}^{M-1} \|\psi_j\|_{L^q(F_j)} \left(\|\Phi - p_{T_{j+1}}\|_{L^p(F_j)} + \|\Phi - p_{T_j}\|_{L^p(F_j)} \right). \end{aligned} \tag{2.25}$$

It then follows from (1.1) and (2.21) that

$$\begin{aligned} \left| \int_{F_z} \psi_z(\Phi - p_T) \, ds \right| \lesssim & h_T^{-(d-1)(1-1/q)} \Big[\|\Phi - p_{T_M}\|_{L^p(F_z)} \\ & + \sum_{j=1}^{M-1} \left(\|\Phi - p_{T_{j+1}}\|_{L^p(F_j)} + \|\Phi - p_{T_j}\|_{L^p(F_j)} \right) \Big]. \end{aligned} \tag{2.26}$$

Then by the Trace Inequality (2.23), shape regularity, and the Bramble-Hilbert Lemma (2.18) (c.f. [11] 4.3.8.) we obtain

$$\begin{aligned} \left| \int_{F_z} \psi_z(\Phi - p_T) \, ds \right| & \lesssim h_T^{-(d-1)(1-1/q)+(\ell-1/p)} \left[|\Phi|_{W_p^\ell(T_M)} + \sum_{j=1}^{M-1} \left(|\Phi|_{W_p^\ell(T_{j+1})} + |\Phi|_{W_p^\ell(T_j)} \right) \right] \\ & \lesssim h_T^{-(d-1)(1-1/q)+(\ell-1/p)} \sum_{\tilde{T} \in \omega_T} |\Phi|_{W_p^\ell(\tilde{T})}, \end{aligned}$$

thus finishing the proof.

Theorem 2.4.5 *Let n denote the degree of the finite element space S_h, and let $1 \leq \ell \leq n+1$, $1 \leq p < \infty$, and $0 \leq k \leq \ell$. For $\Phi \in W_p^1(\omega_T)$ satisfying $\Phi \in W_p^\ell(\tilde{T})$ for all $\tilde{T} \in \omega_T$,*

$$\|I_h\Phi - \Phi\|_{W_p^k(T)} \lesssim h_T^{\ell-k} \sum_{\tilde{T}\in\omega_T} |\Phi|_{W_p^\ell(\tilde{T})}. \tag{2.27}$$

Proof Let p_T be as in Lemma 2.4.4. Then the triangle inequality and (2.22) yield

$$\|I_h\Phi - \Phi\|_{W_p^k(T)} \leq \|\Phi - p_T\|_{W_p^k(T)} + \|I_h(\Phi - p_T)\|_{W_p^k(T)}.$$

Applying the Bramble-Hilbert Lemma to the first term in the right hand side and using (2.20), we obtain

$$\|I_h\Phi - \Phi\|_{W_p^k(T)} \lesssim h_T^{\ell-k}|\Phi|_{W_p^\ell(T)} + \sum_{z\in T} \left| \int_{F_z} \psi_z(\Phi - p_T)\, ds \right| \, \|\varphi_z\|_{W_p^k(T)}.$$

Let $\mathring{\mathcal{N}}_T$ denote the set of interior nodes of T and let $\partial\mathcal{N}_T$ be the set of boundary nodes of T. Then

$$\begin{aligned} \|I_h\Phi - \Phi\|_{W_p^k(T)} \lesssim h_T^{\ell-k}|\Phi|_{W_p^\ell(T)} &+ \sum_{z\in\mathring{\mathcal{N}}_T} \left| \int_{F_z} \psi_z(\Phi - p_T)\, ds \right| \, \|\varphi_z\|_{W_p^k(T)} \\ &+ \sum_{z\in\partial\mathcal{N}_T} \left| \int_{F_z} \psi_z(\Phi - p_T)\, ds \right| \, \|\varphi_z\|_{W_p^k(T)}. \end{aligned} \tag{2.28}$$

Let q be such that $\frac{1}{p} + \frac{1}{q} = 1$ and let d be the dimension of T. Observe that $F_z = T$ for $z \in \mathring{\mathcal{N}}_T$ and the number of nodes $z \in T$ is bounded by a fixed constant $C(n)$ depending on n. We use Hölders inequality, (2.21), (2.22), the Bramble-Hilbert Lemma and $-d(1-1/q) - k + d/p = -k$ to obtain

$$\begin{aligned} \sum_{z\in\mathring{\mathcal{N}}_T} \left| \int_{F_z} \psi_z(\Phi - p_T)\, ds \right| \|\varphi_z\|_{W_p^k(T)} &\lesssim \|\psi_z\|_{L^q(T)} \|\Phi - p_T\|_{L^p(T)} \|\varphi_z\|_{W_p^k(T)} \\ &\lesssim h_T^{-d(1-1/q)-k+d/p} \|\Phi - p_T\|_{L^p(T)} \\ &\lesssim h_T^{\ell-k} |\Phi|_{W_p^\ell(T)}. \end{aligned} \tag{2.29}$$

Lemma (2.4.4) and the fact that the number of nodes of any $T \in \mathcal{T}$ is bounded by $C(n)$ imply that

$$\sum_{z\in\partial\mathcal{N}_T} \left| \int_{F_z} \psi_z(\Phi - p_T)\, ds \right| \, \|\varphi_z\|_{W_p^k(T)} \lesssim h_T^{-(d-1)(1-1/q)+(\ell-1/p)} \sum_{T\in\omega_T} |\Phi|_{W_p^\ell(T)} \, \|\varphi_z\|_{W_p^k(T)}.$$

(2.22) applied to $\|\varphi_z\|_{W_p^k(T)}$, $-(d-1)(1-1/q) + (\ell - 1/p) - k + d/p = \ell - k$, and

shape regularity yield

$$\sum_{z\in\partial\mathcal{N}_T}\left|\int_{F_z}\psi_z(\Phi-p_T)\,ds\right|\;\|\varphi_z\|_{W_p^k(T)}\lesssim h_T^{\ell-k}\sum_{T\in\omega_T}|\Phi|_{W_p^\ell(T)}. \tag{2.30}$$

We substitute (2.29) and (2.30) into (2.28) to obtain (2.27), finishing the proof.

The following are scaled versions of standard Sobolev embedding theorems; cf. [1] Theorem 4.12. We only consider ranges of indices used in our proofs below.

Lemma 2.4.6 *Assume that* $1\le p_1<\frac{d-1}{d-2}$, $1\le p_2<\frac{d}{d-2}$ *and either* $m=2$ *and* $s=1$ *or* $m=1$ *and* $\frac{dp_j}{d+p_j}\le s<\frac{d}{d-1}$, $s\le p_j$ *for* $j=\{1,2\}$. *Then*

$$\|\Phi\|_{L^{p_1}(\partial T)}\lesssim\sum_{j=0}^{m}h_T^{j-d/s+(d-1)/p_1}|\Phi|_{W_s^j(T)},\ \textit{for}\ \Phi\in W_s^j(T), \tag{2.31a}$$

$$\|\Phi\|_{L^{p_2}(T)}\lesssim\sum_{j=0}^{m}h_T^{j-d/s+d/p_2}|\Phi|_{W_s^j(T)},\ \textit{for}\ \Phi\in W_s^j(T). \tag{2.31b}$$

In the following sections we apply our approximation results in the following form.

Corollary 2.4.7 *Assume that either* $p_1=p_2=s=2$ *and* $m=1$ *or* $m=2$, *or that* p_1, p_2, s, *and* m *are related as in Lemma 2.4.6 above. Then for* $T\in\mathcal{T}$,

$$\|I_h\Phi-\Phi\|_{L^{p_1}(\partial T)}\lesssim h_T^{m-d/s+(d-1)/p_1}\sum_{T_i\in\omega_T}|\Phi|_{W_s^m(T_i)}, \tag{2.32a}$$

$$\|I_h\Phi-\Phi\|_{L^{p_2}(T)}\lesssim h_T^{m-d/s+d/p_2}\sum_{T_i\in\omega_T}|\Phi|_{W_s^m(T_i)}. \tag{2.32b}$$

In addition, for $1\le p\le\infty$

$$\|I_h\Phi\|_{L^p(T)}\lesssim\sum_{T_i\in\omega_T}\left(\|\Phi\|_{L^p(T_i)}+h_T\|\nabla\Phi\|_{L^p(T_i)}\right). \tag{2.33}$$

Proof We easily verify (2.32) by combining Theorem 2.4.5 and (2.31). (2.33) follows from the triangle inequality and Theorem 2.4.5.

2.4.4 A generalized Bramble-Hilbert Lemma

In [53] a Bramble-Hilbert Lemma is applied over element patches in order to prove approximation properties for the Scott-Zhang interpolant. Employing the same notation as above, let $0\le j\le n$, $0\le\ell\le n+1$, and $u\in W_p^\ell(\omega_T)$ with $1\le p<\infty$.

Then

$$\inf_{v\in S_h} |u-v|_{W_p^j(\omega_T)} \leq \inf_{p\in\mathbb{P}_n} |u-p_T|_{W_p^j(\omega_T)} \lesssim h_T^{\ell-j}|u|_{W_p^\ell(\omega_T)}. \tag{2.34}$$

Lemma 2.4.4 and Theorem 2.4.5 may be rewritten as a Bramble-Hilbert lemma for broken Sobolev spaces. Let $0 \leq j \leq n$, $k = \max\{j, 1\}$, $1 \leq \ell \leq n+1$, $u \in W_p^1(\omega_T)$, and $u \in W_p^\ell(T')$ for each $T' \subset \omega_T$. Then

$$\begin{aligned}\inf_{v\in S_h} \left(\sum_{T'\subset\omega_T} |u-v|^p_{W_p^j(T')}\right)^{1/p} &\lesssim \left(\sum_{T'\subset\omega_T} \inf_{p_{T'}\in\mathbb{P}_n} h_T^{k-j}|u-p_{T'}|^p_{W_p^k(T')}\right)^{1/p}, \\ &\lesssim h_T^{\ell-j}\left(\sum_{T'\subset\omega_T} |u|^p_{W_p^\ell(T')}\right)^{1/p}.\end{aligned} \tag{2.35}$$

The two differences between (2.34) and (2.35) are that the former uses standard and the latter broken Sobolev spaces, and that (2.35) requires $k, \ell \geq 1$. Theorem 3.2 of [58] establishes that continuous and discontinuous finite element spaces yield equivalent approximation in the H^1 seminorm not only asymptotically but on any mesh satisfying reasonable assumptions; this is essentially the first inequality in (2.35) with $p = 2$ and $j = k = 1$. We thus again emphasize that we apply techniques in [58] in a different context but with only modest generalization of the basic ideas.

THIS PAGE INTENTIONALLY LEFT BLANK

Chapter 3

A posteriori error estimates for elliptic equations

This chapter contains results that we proved in [12]. We present new efficient L^2 and pointwise a posteriori error estimates for the Laplace-Beltrami equation (2.8). Some interesting applications that make use of this type of estimates include solutions for the Allen-Cahn equation [6], [26] among others.

3.1 Model problem

We consider the model elliptic surface PDE

$$-\Delta_\Gamma u = f \text{ on } \Gamma. \tag{3.1}$$

Throughout we consider (3.1) while assuming $\int_\Gamma u \ \mathrm{d}\sigma = \int_\Gamma f \ \mathrm{d}\sigma = 0$ in order to ensure existence and uniqueness of solutions. Here Γ is a C^3 closed (i.e. $\partial\Gamma = \emptyset$), two-dimensional surface Γ embedded in $\mathbb{R}^3$; extension to higher-dimensional surfaces of codimension one is mostly immediate.

3.1.1 Finite element approximation

A canonical surface finite element method (SFEM) was defined in [24]. This is the method we consider throughout, though extension to higher order FEM and surface approximations could also be considered [19, 42]. The weak form of (3.1) is: find $u \in H^1(\Gamma)$ such that $\int_\Gamma u \ \mathrm{d}\sigma = 0$ and

$$\int_\Gamma \nabla_\Gamma u \nabla_\Gamma v \ d\sigma = \int_\Gamma f v \ d\sigma \ \forall \ v \in H^1(\Gamma). \tag{3.2}$$

Denote by $f_h(x)$ an approximation of f over Γ_h satisfying $\int_{\Gamma_h} f_h = 0$, for example, $f_h(x) = \mu_h f(a(x)), x \in \Gamma_h$. Let S_h denote the finite element space of piecewise polynomials defined over the faces of Γ_h. Our finite element method produces $u_h \in S_h$ that solves the problem

$$\int_{\Gamma_h} \nabla_{\Gamma_h} u_h \nabla_{\Gamma_h} v_h \ d\sigma_h = \int_{\Gamma_h} f_h v_h \ d\sigma_h \ \forall \ v_h \in S_h. \tag{3.3}$$

3.1.2 Comparison of Sobolev norms on discrete and continuous surfaces

Our main results are proved by duality arguments involving dual functions lying in W_p^2 Sobolev spaces. [24] contains a brief comparison of W_p^2 Sobolev norms of functions on Γ and their extensions to Γ_h. We give a more precise statement about the geometric dependencies of these relationships.

Lemma 3.1.1 *Let $T \in \mathcal{T}$ and $v \in W_p^2(a(T))$ for some $1 \le p \le \infty$. Then*

$$\begin{aligned} |v^\ell|_{W_p^2(T)} \le \left\| \frac{1}{\mu_h} \right\|_{L^\infty(T)}^{1/p} \Big(& \|\mathbf{P}_h[\mathbf{I} - d\mathbf{H}]\|_{L^\infty(a(T))}^2 |v|_{W_p^2(a(T))} \\ & + \Big[\|\mathbf{P_h H}\|_{L^\infty(a(T))} \|\vec{\nu} - (\vec{\nu}\cdot\vec{\nu}_h)\vec{\nu}_h\|_{L^\infty(a(T))} \\ & + \max_{i=1,2,3} \|d\mathbf{P}_h \mathbf{H}_{x_i}\|_{L^\infty(a(T))} \Big] \ |v|_{W_p^1(a(T))} \Big). \end{aligned} \tag{3.4}$$

Before beginning the proof, we mention a couple of notational conventions. First, for vectors a, b, c, d we have $(a \otimes b)(c \otimes d) = (b \cdot c)a \otimes d$. Second, we regard $\nabla v(a(x))$ as a column vector.

Proof By equation (2.10) and the change of variable formula (2.5) we have

$$\begin{aligned} |v^\ell|_{W_p^2(T)} &= \Big\{ \sum_{|\alpha|=2} \int_T [D_h^\alpha (v^\ell(x))]^p d\sigma_h \Big\}^{1/p} \\ &= \Big\{ \sum_{|\alpha|=2} \int_{a(T)} \frac{1}{\mu_h} [D_h^\alpha \left(v(a(x))\right)]^p d\sigma \Big\}^{1/p}. \end{aligned} \tag{3.5}$$

(2.7), (2.3), the chain rule and the fact that the projection matrix $\mathbf{P}_h$ is constant in each triangle yield

$$\begin{aligned} D_h^2(v^\ell(x)) &= \nabla_{\Gamma_h}\{\mathbf{P}_h[\mathbf{P} - d\mathbf{H}]\nabla v(a(x))\} \\ &= \mathbf{P}_h \nabla_{\Gamma_h}\{[\mathbf{P} - d\mathbf{H}]\nabla v(a(x))\} \\ &= \mathbf{P}_h \nabla\{[\mathbf{I} - d\mathbf{H}]\nabla_\Gamma v(a(x))\}\mathbf{P}_h. \end{aligned}$$

Next we expand the right hand side of the previous equation:

$$\begin{aligned} D_h^2(v^\ell(x)) = & \mathbf{P}_h \Big\{ \nabla\nabla_\Gamma v(a(x))[\mathbf{P} - d\mathbf{H}] - \mathbf{H}\nabla_\Gamma v(a(x)) \otimes \vec{\nu} \\ & - d[\mathbf{H}_{x_i}\nabla_\Gamma v(a(x))]_{i=1}^3 - d\mathbf{H}\nabla\nabla_\Gamma v(a(x))[\mathbf{P} - d\mathbf{H}] \Big\}\mathbf{P}_h. \end{aligned} \tag{3.6}$$

Here $\mathbf{H}_{x_i}$ denotes the derivative of $\mathbf{H}$ with respect to x_i, and $[\mathbf{H}_{x_i}\nabla_\Gamma v(a(x))]_{i=1}^3$ is a matrix whose i-th column is given by $\mathbf{H}_{x_i}\nabla_\Gamma v(a(x))$. Regrouping terms then yields

$$\nabla_\Gamma^2 v(a(x))[\mathbf{I} - d\mathbf{H}] - d\mathbf{H}\nabla_\Gamma^2 v(a(x))[\mathbf{I} - d\mathbf{H}] = [\mathbf{I} - d\mathbf{H}]\nabla_\Gamma^2 v(a(x))[\mathbf{I} - d\mathbf{H}].$$

Hence we write

$$\begin{aligned} D_h^2(v^\ell(x)) = & \mathbf{P}_h \Big\{ [\mathbf{I} - d\mathbf{H}]\nabla_\Gamma^2 v(a(x))[\mathbf{I} - d\mathbf{H}] - \mathbf{H}\nabla_\Gamma v(a(x)) \otimes \vec{\nu} \\ & - d[\mathbf{H}_{x_i}\nabla_\Gamma v(a(x))]_{i=1}^3 \Big\}\mathbf{P}_h. \end{aligned} \tag{3.7}$$

Using (3.5), (3.7) and Hölder's inequality we obtain (3.4).

For $p = 2$ Lemma 3.1.1 has the same form as Lemma 3 in [24], which states that $|v^\ell|_{H^2(T)} \leq C\Big\{h_T|v|_{H^1(a(T))} + |v|_{H^2(a(T))}\Big\}$. The difference is that Lemma 3.1.1 includes explicit geometric information about the constant. We quickly verify that using equation (3.4) we get Lemma 3 of [24]. Because $\Gamma \in C^3$, $\|\mathbf{P}_h[\mathbf{I} - d\mathbf{H}]\|_{L^\infty(a(T))} \lesssim 1$ in (3.4). From (2.4) and $\Gamma \in C^3$ it follows that the term multiplying $|v|_{W^1_p(a(T))}$ is of order h_T, reducing to the statement of [24] Lemma 3.

3.2 L^2 a posteriori estimate

In this section we derive an L^2 a posteriori error estimate. We first state a standard regularity result.

Lemma 3.2.1 *Regularity (c.f. [19] Lemma 2.1). Let $f \in L^2(\Gamma)$ satisfy $\int_\Gamma f \, d\sigma = 0$, and assume that Γ is a C^2 surface. Then the problem $L(u, v) = (f, v)\ \forall\ v \in H^1(\Gamma)$ has a unique weak solution satisfying $\int_\Gamma u \, d\sigma = 0$ and*

$$\|u\|_{H^2(\Gamma)} \leq C\|f\|_{L^2(\Gamma)}. \tag{3.8}$$

We next define the error $e := u - u_h^\ell$. From this point on v_h will be used to denote the interpolant of v^ℓ, i.e. $v_h \equiv I_h v^\ell$. Our main result is stated in the following theorem.

Theorem 3.2.2 *Let $u(x)$ be the solution to (3.1), assume that Γ is a C^3 surface, and define*

$$\begin{aligned}
C_p(K) &:= \left\| \frac{1}{\mu_h} \right\|^{1/p}_{L^\infty(K)}, \qquad C_p(\omega_K) = \left\| \frac{1}{\mu_h} \right\|^{1/p}_{L^\infty(\omega_K)} \\
\theta_p(K) &:= C_p(K)\Big(\|\mathbf{P}_h[\mathbf{I} - d\mathbf{H}]\|^2_{L^\infty(a(K))} \\
&\quad + \|\mathbf{P_h H}\|_{L^\infty(a(K))} \|\vec{\nu} - (\vec{\nu}\cdot\vec{\nu}_h)\vec{\nu}_h\|_{L^\infty(a(T))} \\
&\quad + \max_{i=1,2,3} \|d\mathbf{P}_h\mathbf{H}_{x_i}\|_{L^\infty(a(K))}\Big), \\
\theta_p(\omega_K)^p &= \sum_{K'\subset\omega_K} \theta_p(K')^p,\ 1 \leq p < \infty, \qquad \theta_\infty(\omega_K) = \max_{K'\subset\omega_K} \theta_\infty(K') \\
\gamma_2(K) &= C_2(K)(1 + h_T\|\mathbf{P} - d\mathbf{H}\|_{L^\infty(K)}), \qquad \gamma_2(\omega_K)^2 = \sum_{K'\subset\omega_K} \gamma_2(K')^2.
\end{aligned} \tag{3.9}$$

Then the following bound holds:

$$\begin{aligned}\|u-u_h^\ell\|_{L^2(\Gamma)} \lesssim \Big[\sum_{T\in\mathcal{T}}\Big(\theta_2(\omega_T)^2\Big\{h_T^4\|\mu_h f^\ell+\triangle_{\Gamma_h}u_h\|^2_{L^2(T)}\\ +h_T^3\|[\![\nabla_{\Gamma_h}u_h]\!]\|^2_{L^2(\partial T)}\Big\}+\|[(\mathbf{P}-\mathbf{A}_h^\ell)\nabla_\Gamma u_h^\ell]\|^2_{L^2(a(T))}\\ +\|u_h^\ell-\mu_h u_h^\ell\|^2_{L^2(a(T))}+\gamma_2(\omega_T)^2\|\mu_h f^\ell-f_h\|^2_{L^2(T)}\Big]^{1/2}.\end{aligned} \tag{3.10}$$

The constant hidden in "$\lesssim$" depends on the regularity constant in (3.8) *but not other essential quantities.*

We use the following lemma to prove Theorem 3.2.2.

Lemma 3.2.3 *Let u and u_h^ℓ be the continuous and discrete solutions of* (3.1) *respectively. Let v solve $-\triangle_\Gamma v = u-\mu_h u_h^\ell$ in Γ, $\int_\Gamma v\,d\sigma=0$. Then the following bound holds:*

$$\|u-u_h^\ell\|^2_{L^2(\Gamma)} \lesssim I+II+III+IV+\|\mu_h u_h^\ell-u_h^\ell\|^2_{L^2(\Gamma)}, \tag{3.11}$$

where

$$\begin{aligned} I&=\int_{\Gamma_h}(\mu_h f^\ell+\triangle_{\Gamma_h}u_h)(v^\ell-v_h)\,d\sigma_h, \qquad II=-\int_\Gamma[(\mathbf{P}-\mathbf{A}_h^\ell)\nabla_\Gamma u_h^\ell]\cdot\nabla_\Gamma v\,d\sigma,\\ III&=-\frac{1}{2}\sum_{T\in\mathcal{T}}\int_{\partial T}[\![\nabla_{\Gamma_h}u_h]\!](v^\ell-v_h)\,ds, \qquad IV=\int_{\Gamma_h}(\mu_h f^\ell-f_h)v_h\,d\sigma_h.\end{aligned}$$

Proof Since $\int_\Gamma u=0$ and $\int_{\Gamma_h}u_h=0$, it follows that $\int_\Gamma(u-\mu_h u_h^\ell)\,d\sigma=0$. Now we compute the L^2 norm of the error by

$$\begin{aligned}\|u-u_h^\ell\|^2_{L^2(\Gamma)}&=(u-u_h^\ell,u-\mu_h u_h^\ell+\mu_h u_h^\ell-u_h^\ell)\\ &=(u-u_h^\ell,-\triangle_\Gamma v)+(u-u_h^\ell,\mu_h u_h^\ell-u_h^\ell)=A+(u-u_h^\ell,\mu_h u_h^\ell-u_h^\ell),\end{aligned} \tag{3.12}$$

where $A=(u-u_h^\ell,-\triangle_\Gamma v)$. By integration by parts we get since $\partial\Gamma=\emptyset$:

$$A=(u-u_h^\ell,-\triangle v)=\int_\Gamma\nabla_\Gamma(u-u_h^\ell)\nabla_\Gamma v\,d\sigma. \tag{3.13}$$

The residual identity given in equation (3.5) of [20] gives us

$$\begin{aligned} A = \int_\Gamma \nabla_\Gamma(u - u_h^\ell)\nabla_\Gamma v \; d\sigma = &\int_{\Gamma_h} (\mu_h f^\ell + \triangle_{\Gamma_h} u_h)(v^\ell - v_h) \; d\sigma_h \\ &- \int_\Gamma [(\mathbf{P} - \mathbf{A}_h^\ell)\nabla_\Gamma u_h^\ell] \cdot \nabla_\Gamma v \; d\sigma \\ &- \frac{1}{2}\sum_{T\in\mathcal{T}} \int_{\partial T} [\![\nabla_{\Gamma_h} u_h]\!](v^\ell - v_h) \; ds \\ &+ \int_{\Gamma_h} (\mu_h f^\ell - f_h) v_h \; d\sigma_h \\ =&I + II + III + IV. \end{aligned} \tag{3.14}$$

Combining equations (3.12) and (3.14) we easily get for any $\varepsilon > 0$

$$\begin{aligned} \|u - u_h^\ell\|_{L^2(\Gamma)}^2 &\leq I + II + III + IV + \|u - u_h^\ell\|_{L^2(\Gamma)} \|\mu_h u_h^\ell - u_h^\ell\|_{L^2(\Gamma)} \\ &\leq I + II + III + IV + \frac{\varepsilon}{2}\|u - u_h^\ell\|_{L^2(\Gamma)}^2 + \frac{1}{2\varepsilon}\|\mu_h u_h^\ell - u_h^\ell\|_{L^2(\Gamma)}^2. \end{aligned} \tag{3.15}$$

Taking $\varepsilon = \frac{1}{2}$ and rescaling concludes the proof of the Lemma.

3.2.1 A posteriori upper bound (Proof of Theorem 3.2.2)

We now prove bounds for elements I through IV of (3.14).
Bound for I. Hölder's inequality yields

$$\begin{aligned} I &= \int_{\Gamma_h} |(\mu_h f^\ell + \triangle_{\Gamma_h} u_h)(v^\ell - v_h)| \; d\sigma_h \\ &\leq \sum_{T\in\mathcal{T}} \|\mu_h f^\ell + \triangle_{\Gamma_h} u_h\|_{L^2(T)} \|v^\ell - v_h\|_{L^2(T)}. \end{aligned} \tag{3.16}$$

Recall that we defined $v_h = I_h v^\ell$. Then by (2.32b) with $p = s = m = 2$ we get

$$\|v^\ell - v_h\|_{L^2(T)} \lesssim h_T^2 \sum_{K\in\omega_T} |v^\ell|_{H^2(K)}. \tag{3.17}$$

Next we apply Lemma 3.1.1, (3.9), and observe that $\|\cdot\|_{H^2(T)}$ bounds the H^1 and H^2 semi-norms to get $\sum_{K\in\omega_T} |v^\ell|_{H^2(K)} \lesssim \theta_2(\omega_T)\|v\|_{H^2(a(\omega_T))}$. Finite overlap of the patches ω_T then yields

$$I \lesssim \left(\sum_{T\in\mathcal{T}} h_T^4 \|\mu_h f^\ell + \triangle_{\Gamma_h} u_h\|_{L^2(T)}^2 \theta_2(\omega_T)^2\right)^{1/2} \|v\|_{H^2(\Gamma)}. \tag{3.18}$$

Bound for II. The Cauchy-Schwarz inequality and $\|v\|_{H^1(\Gamma)} \leq \|v\|_{H^2(\Gamma)}$ yields

$$\begin{aligned} II &= \int_\Gamma [(\mathbf{P} - \mathbf{A}_h^\ell)\nabla_\Gamma u_h^\ell] \cdot \nabla_\Gamma v \; d\sigma \\ &\leq \|[(\mathbf{P} - \mathbf{A}_h^\ell)\nabla_\Gamma u_h^\ell]\|_{L^2(\Gamma)} \|\nabla_\Gamma v\|_{L^2(\Gamma)} \\ &= \left\{ \sum_{T \in \mathcal{T}} \|[(\mathbf{P} - \mathbf{A}_h^\ell)\nabla_\Gamma u_h^\ell]\|^2_{L^2(a(T))} \right\}^{1/2} \|v\|_{H^2(\Gamma)}. \end{aligned} \tag{3.19}$$

Bound for III. Using Hölder's inequality, (2.32a) with $p = s = m = 2$, and computing as in (3.19) yields

$$\begin{aligned} III &= \sum_{T \in \mathcal{T}} \int_{\partial T} [\![\nabla_{\Gamma_h} u_h]\!](v^\ell - v_h) \; ds \\ &\leq \sum_{T \in \tau} \|[\![\nabla_{\Gamma_h} u_h]\!]\|_{L^2(\partial T)} \|v^\ell - v_h\|_{L^2(\partial T)} \\ &\lesssim \sum_{T \in \mathcal{T}} \|[\![\nabla_{\Gamma_h} u_h]\!]\|_{L^2(\partial T)} h_T^{3/2} \sum_{K \in \omega_T} |v^\ell|_{H^2(K)} \\ &\lesssim \left(\sum_{T \in \mathcal{T}} \|[\![\nabla_{\Gamma_h} u_h]\!]\|^2_{L^2(\partial T)} h_T^3 \theta_2(\omega_T)^2 \right)^{1/2} \|v\|_{H^2(\Gamma)}. \end{aligned} \tag{3.20}$$

Bound for IV. It follows from Hölder's inequality and (2.33) that

$$\begin{aligned} IV &= \int_{\Gamma_h} |(\mu_h f^\ell - f_h) v_h| \; d\sigma_h \\ &\leq \sum_{T \in \mathcal{T}} \|(\mu_h f^\ell - f_h)\|_{L^2(T)} \|v_h\|_{L^2(T)} \\ &\lesssim \sum_{T \in \mathcal{T}} \|\mu_h f^\ell - f_h\|_{L^2(T)} \sum_{K \in \omega_T} (\|v^\ell\|_{L^2(K)} + h_T \|\nabla_\Gamma v^\ell\|_{L^2(K)}). \end{aligned} \tag{3.21}$$

Then we use (2.3), (2.5), (2.33) and Hölder's inequality to deduce that

$$\begin{aligned} \int_{\Gamma_h} |(\mu_h f^\ell - f_h) v_h| \; d\sigma_h &\lesssim \sum_{T \in \mathcal{T}} \big[\|\mu_h f^\ell - f_h\|_{L^2(T)} \sum_{K \in \omega_T} C_2(K) (\|v\|_{L^2(a(K))} \\ &\quad + h_T \|(\mathbf{I} - d\mathbf{H})\nabla v\|_{L^2(a(K))}) \big] \\ &\lesssim \sum_{T \in \mathcal{T}} \gamma_2(\omega_T) \|\mu_h f^\ell - f_h\|_{L^2(T)} \|v\|_{H^2(a(K))} \\ &\lesssim \left(\sum_{T \in \mathcal{T}} \gamma_2(\omega_T)^2 \|\mu_h f^\ell - f_h\|^2_{L^2(T)} \right)^{1/2} \|v\|_{H^2(\Gamma))}. \end{aligned} \tag{3.22}$$

Bound for (3.14). Let

$$\begin{aligned}\eta^2 =& \sum_{T\in\mathcal{T}} h_T^4 \|\mu_h f^\ell + \triangle_{\Gamma_h} u_h\|^2_{L^2(T)} \theta_2(\omega_T)^2 + \|[(\mathbf{P}-\mathbf{A}_h^\ell)\nabla_\Gamma u_h^\ell]\|^2_{L^2(\Gamma)} \\ &+ \sum_{T\in\mathcal{T}} \|[\![\nabla_{\Gamma_h} u_h]\!]\|^2_{L^2(\partial T)} h_T^3 \theta_2(\omega_T)^2 + \sum_{T\in\mathcal{T}} \gamma_2(\omega_T)^2 \|\mu_h f^\ell - f_h\|^2_{L^2(T)}.\end{aligned} \tag{3.23}$$

Using (3.18), (3.19), (3.20) and (3.22), and the regularity result (3.8) yields

$$I + II + III + IV \lesssim \eta \|u - \mu_h u_h^\ell\|_{L^2(\Gamma)}. \tag{3.24}$$

We combine (3.24), (3.14), (3.11) and then use Cauchy and the triangle inequality to get

$$\begin{aligned}\|u-u_h^\ell\|^2_{L^2(\Gamma)} &\lesssim \eta\|u-\mu_h u_h^\ell\|_{L^2(\Gamma)} + \|u_h^\ell - \mu_h u_h^\ell\|^2_{L^2(\Gamma)} \\ &\leq \frac{1}{4\epsilon}\eta^2 + \epsilon\|u-\mu_h u_h^\ell\|^2_{L^2(\Gamma)} + \|u_h^\ell - \mu_h u_h^\ell\|^2_{L^2(\Gamma)} \\ &\leq \frac{1}{4\epsilon}\eta^2 + 2\epsilon\|u-u_h^\ell\|^2_{L^2(\Gamma)} + 2\epsilon\|u_h^\ell - \mu_h u_h^\ell\|^2_{L^2(\Gamma)} + \|u_h^\ell - \mu_h u_h^\ell\|^2_{L^2(\Gamma)}.\end{aligned}$$

Rearranging terms and taking ϵ sufficiently small write finalizes the proof of Theorem 3.2.2. □

We define the error indicator $\hat{\eta}(T)$ in each triangle $T \in \mathcal{T}$ as follows:

$$\begin{aligned}\hat{\eta}(T) :=& \Big\{ h_T^2 \|\mu_h f^\ell + \triangle_{\Gamma_h} u_h\|_{L^2(T)} + h_T^{3/2} \|[\![\nabla_{\Gamma_h} u_h]\!]\|_{L^2(\partial T)} \Big\} \theta_2(\omega_T) \\ &+ \|[(\mathbf{P}-\mathbf{A}_h^\ell)\nabla_\Gamma u_h^\ell]\|_{L^2(a(T))} + \|u_h^\ell - \mu_h u_h^\ell\|_{L^2(a(T))} \\ &+ \gamma_2(\omega_T)\|\mu_h f^\ell - f_h\|_{L^2(T)}.\end{aligned} \tag{3.25}$$

Thus we write $\|u-u_h^\ell\|_{L^2(\Gamma)} \lesssim \left(\sum_{T\in\mathcal{T}} \hat{\eta}^2(T)\right)^{1/2}$.

3.2.2 Efficiency

Next we verify that the residual part of the estimator (3.25) is bounded above by the true error plus data oscillation and geometric terms. We use standard techniques developed in [59].

We start by defining and describing geometric constants that arise when we move from Γ_h to Γ.

Lemma 3.2.4 *Assume that $T \in \mathcal{T}$ and γ is an edge of T. Let $\mathcal{P}$ be the piecewise constants on $\mathcal{T}$. For $x \in \Gamma_h$ let $\tilde{x} = a(x)$, $\tilde{v_h}(a(x)) = v_h(x)$, and $\tilde{T} = a(T)$. Let ϕ_T, ϕ_γ be the squares of the interior bubble function associated with T and the edge bubble function associated with γ respectively and define*

$$\mathcal{G} := [\mathbf{I} - d\mathbf{H}]^{-1}\left[I - \frac{\vec{\nu}_h \otimes \vec{\nu}}{\vec{\nu}_h \cdot \vec{\nu}}\right]. \tag{3.26}$$

Then for $v_h \in \mathcal{P}$ and $1 \leq p \leq \infty$

$$\|\triangle_\Gamma(\tilde{\phi_T}\tilde{v}_h)\|_{L^p(\tilde{T})} \leq \left(h_T^{-2}\|\mathcal{G}\|_{L^\infty(T)} + h_T^{-1}\|D\mathcal{G}\|_{L^\infty(T)}\right)\|v\|_{L^p(T)}, \tag{3.27a}$$

$$\|\triangle_\Gamma(\tilde{\phi_\gamma}\tilde{v}_h)\|_{L^p(\tilde{T})} \leq \left(h_T^{-2+1/p}\|\mathcal{G}\|_{L^\infty(T)} + h_T^{-1+1/p}\|D\mathcal{G}\|_{L^\infty(T)}\right)\|v\|_{L^p(\gamma)}. \tag{3.27b}$$

Proof Let $w := \phi_T v$. (2.8) yields $\triangle_\Gamma \tilde{w} = \nabla \cdot \nabla_\Gamma \tilde{w} - \vec{\nu}[D\nabla_\Gamma \tilde{w}]\vec{\nu}^T$. We apply [20] equation 2.19 to this equation. Let e_i denote the column unit vector with entry-i equal to one and zero everywhere else, let $[(\cdot)_i]$, $1 \leq i \leq 3$ denote a matrix where the i-th column is given by $(\cdot)_i$, and calculate

$$\begin{aligned}
\triangle_\Gamma \tilde{w} =& \nabla \cdot (\mathcal{G}\nabla_{\Gamma_h} w) - \vec{\nu}\left[D\left(\mathcal{G}\nabla_{\Gamma_h} w\right)\right]\vec{\nu}^T \\
=& \sum_{i=1}^{3}\left(e_i^T \mathcal{G}\partial_{x_i}(\nabla_{\Gamma_h} w)\right) - \vec{\nu}\left[\mathcal{G}\partial_{x_i}(\nabla_{\Gamma_h} w)\right]_{i=1}^{3}\vec{\nu}^T \\
&+ \sum_{i=1}^{3}\left(e_i^T \partial_{x_i}\left(\mathcal{G}\right)\nabla_{\Gamma_h} w\right) - \vec{\nu}\left[\partial_{x_i}\left(\mathcal{G}\right)\nabla_{\Gamma_h} w\right]_{i=1}^{3}\vec{\nu}^T.
\end{aligned}$$

Taking the L^p norm of both sides and using the triangle and Hölder's inequalities yields

$$\begin{aligned}
\|\triangle_\Gamma w\|_{L^p(\tilde{T})} \leq& \sum_{i=1}^{3}\left(\|e_i^T\mathcal{G}\|_{L^\infty(T)}\|\partial_{x_i}\nabla_{\Gamma_h} w\|_{L^p(T)} + \|e_i^T\partial_{x_i}\mathcal{G}\|_{L^\infty(T)}\|\nabla_{\Gamma_h} w\|_{L^p(T)}\right) \\
&+ \|\vec{\nu}\mathcal{G}\|_{L^\infty(T)}\|D(\nabla_{\Gamma_h} w)\vec{\nu}^T\|_{L^p(T)} + \|D\mathcal{G}\|_{L^\infty}\|\nabla_{\Gamma_h} w\|_{L^p(T)},
\end{aligned}$$

thus

$$\|\triangle_\Gamma w\|_{L^p(\tilde{T})} \lesssim \|\mathcal{G}\|_{L^\infty(T)}|\phi_T v|_{W_p^2(T)} + \|D\mathcal{G}\|_{L^\infty(T)}|\phi_T v|_{W_p^1(T)}.$$

Because v is constant in each T we can use an inverse estimate to deduce (3.27a). The same argument, after observing that we apply a scaling argument to go from T to γ, yields (3.27b).

We are ready to prove the following efficiency result.

Lemma 3.2.5 *Let $\bar{f}$ be an elementwise constant approximation to f. Let $1 \leq q \leq \infty$, $f \in L_q(\Gamma)$. For $x \in \Gamma_h$ let $\tilde{x} = a(x)$, $\tilde{v_h}(a(x)) = v_h(x)$, choose $\mu_h f^\ell = f_h$, and let $\mathcal{G}$ be defined by equation* (3.26)*. Then*

$$\begin{aligned}
h_T^2\|\mu_h f^\ell + \triangle_{\Gamma_h} u_h\|_{L^q(T)} &+ h_T^{1+1/q}\|[\![\nabla_{\Gamma_h} u_h]\!]\|_{L^q(\partial T)} \\
\lesssim& \|e\|_{L^q(\tilde{\omega}_T)}(\|\mathcal{G}\|_{L^\infty(\omega_T)} + h_T\|D\mathcal{G}\|_{L^\infty(\omega_T)}) \\
&+ h_T\|\mathcal{G}\|_{L^\infty(\omega_T)}\|(\mathbf{P} - \mathbf{A}_h^\ell)\nabla_\Gamma u_h^\ell\|_{L^q(\tilde{\omega}_T)} + h_T^2\|\mu_h f^\ell - \bar{f}\|_{L^q(\omega_T)}.
\end{aligned} \tag{3.28}$$

We observe that (3.28) does not contain all the geometric terms of (3.25). The omission of this terms simplifies the analysis and does not affect the understanding of

the efficiency result. It is discussed in [8] that while the efficiency estimates, for the residual component of the error estimator, play an important role in understanding convergence and optimality for ASFEM, the efficiency of the geometric components does not.

Proof We introduce a more compact notation for the residuals:

$$r := \mu_h f^\ell + \triangle_{\Gamma_h} u_h, \qquad R := -[\![\nabla_{\Gamma_h} u_h]\!]. \tag{3.29}$$

and define

$$\mathcal{G}_1 := h_T^{-2}\|\mathcal{G}\|_{L^\infty(T)} + h_T^{-1}\|D\mathcal{G}\|_{L^\infty(T)}. \tag{3.30}$$

Let $\bar{r}$ and $\bar{R}$ denote piecewise constant approximations of r and R respectively. We choose p such that $\frac{1}{p}+\frac{1}{q}=1$, use the residual equation (3.14) and let $v = \tilde{\phi_T}\tilde{\bar{r}}$, $v_h = 0$. Since ϕ_T and $\nabla_{\Gamma_h}\phi_T$ vanish on ∂T we obtain

$$\int_{\tilde{T}} \nabla_\Gamma e \nabla_\Gamma(\tilde{\phi_T}\tilde{\bar{r}})\, d\sigma = \int_T \phi_T r \bar{r}\, d\sigma_h - \int_{\tilde{T}} (\mathbf{P} - \mathbf{A}_h^\ell)\nabla_\Gamma u_h^\ell \nabla_\Gamma(\tilde{\phi_T}\tilde{\bar{r}})\, d\sigma.$$

Thus after adding and subtracting the appropriate terms and rearranging we get

$$\int_T \phi_T \bar{r}^2\, d\sigma_h = \int_{\tilde{T}} (\nabla_\Gamma e + (\mathbf{P} - \mathbf{A}_h^\ell)\nabla_\Gamma u_h^\ell)\nabla_\Gamma(\tilde{\phi_T}\tilde{\bar{r}})\, d\sigma + \int_T \phi_T \bar{r}(\bar{r} - r)\, d\sigma_h. \tag{3.31}$$

Integration by parts together with Lemma 3.2.4 and (3.30) gives

$$\begin{aligned}
\int_{\tilde{T}} \nabla_\Gamma e \nabla_\Gamma(\tilde{\phi_T}\tilde{\bar{r}})\, d\sigma =& \int_{\tilde{T}} -e\triangle_\Gamma(\tilde{\phi_T}\tilde{\bar{r}})\, d\sigma \\
\leq& \|e\|_{L^q(\tilde{T})}\|\triangle_\Gamma \tilde{\phi_T}\tilde{\bar{r}}\|_{L^p(\tilde{T})} \\
\leq& \|e\|_{L^q(\tilde{T})}\left(h_T^{-2}\|\mathcal{G}\|_{L^\infty(T)} + h_T^{-1}\|D\mathcal{G}\|_{L^\infty(T)}\right)\|\bar{r}\|_{L^p(T)} \\
=& \mathcal{G}_1\|e\|_{L^q(\tilde{T})}\|\bar{r}\|_{L^p(T)}.
\end{aligned} \tag{3.32}$$

In a similar way we apply Hölder's inequality, use [20] equation 2.19 together with the definition of $\mathcal{G}$, [3] Lemma 2.1 and Theorem 2.2 to obtain

$$\begin{aligned}
&\int_{\tilde{T}} (\mathbf{P} - \mathbf{A}_h^\ell)\nabla_\Gamma u_h^\ell \nabla_\Gamma(\tilde{\phi_T}\tilde{\bar{r}})\, d\sigma \\
&\qquad \leq \|\mathcal{G}\|_{L^\infty(T)}\|(\mathbf{P} - \mathbf{A}_h^\ell)\nabla_\Gamma u_h^\ell\|_{L^q(\tilde{T})}\|\nabla_{\Gamma_h}(\phi_T\bar{r})\|_{L^p(T)} \\
&\qquad \lesssim h_T^{-1}\|\mathcal{G}\|_{L^\infty(T)}\|(\mathbf{P} - \mathbf{A}_h^\ell)\nabla_\Gamma u_h^\ell\|_{L^q(\tilde{T})}\|\bar{r}\|_{L^p(T)}.
\end{aligned} \tag{3.33}$$

We combine (3.31), (3.32) and (3.33) to get

$$\begin{aligned}
\int_T \phi_T \bar{r}^2\, d\sigma_h \leq& \|\bar{r}\|_{L^p(T)}\big\{\mathcal{G}_1\|e\|_{L^q(\tilde{T})} + h_T^{-1}\|\mathcal{G}\|_{L^\infty(T)}\|(\mathbf{P} - \mathbf{A}_h^\ell)\nabla_\Gamma u_h^\ell\|_{L^q(\tilde{T})} \\
&+ \|\bar{r} - r\|_{L^q(T)}\big\}.
\end{aligned} \tag{3.34}$$

It follows from [3] Lemma 2.1 that $\|\bar{r}\|^2_{L^2(T)} \lesssim \int_T \phi_T \bar{r}^2 \, d\sigma_h$. Let d be the dimension of the simplex T. The equivalence of norms in a finite dimensional space and a scaling argument gives the bound $h_T^{-d/p+d/2}\|\bar{r}\|_{L^p(T)} \lesssim \|\bar{r}\|_{L^2(T)}$. Thus we have $h_T^{d-d(1/p+1/q)}\|\bar{r}\|_{L^p(T)}\|\bar{r}\|_{L^q(T)} \lesssim \|\bar{r}\|^2_{L^2(T)}$. Observe that $d - d(1/p + 1/q) = 0$ and finally apply the triangle inequality to $\|\bar{r}\|_{L^q(T)}$ to obtain

$$\|r\|_{L^q(T)} \leq \mathcal{G}_1\|e\|_{L^q(\tilde{T})} + h_T^{-1}\|\mathcal{G}\|_{L^\infty(T)}\|(\mathbf{P} - \mathbf{A}_h^\ell)\nabla_\Gamma u_h^\ell\|_{L^q(\tilde{T})} + \|\bar{r} - r\|_{L^q(T)}. \quad (3.35)$$

Let γ be an edge of T, $v := \tilde{\phi_\gamma}\tilde{\bar{R}}$, $v_h = 0$, and $\mu_h f^\ell = f_h$. Let $\omega_\gamma := \{T \in \mathcal{T} | T \cap \gamma \neq \emptyset\}$ and observe that ϕ_γ vanishes outside of ω_γ. Then it follows from (3.14) that

$$\begin{aligned}\int_\gamma \bar{R}^2 \, ds \lesssim \int_\gamma \phi_\gamma \bar{R}^2 \, ds = \int_{\tilde{\omega_\gamma}} (\nabla_\Gamma e + (\mathbf{P} - \mathbf{A}_h^\ell)\nabla_\Gamma u_h^\ell)\nabla_\Gamma(\phi_\gamma^\ell \tilde{\bar{R}}) \, d\sigma - \int_{\omega_\gamma} \phi_\gamma r \bar{R} \, d\sigma_h \\ + \int_\gamma \phi_\gamma \bar{R}(\bar{R} - R) \, d\sigma.\end{aligned}$$

Following the steps used to derive (3.35) we use Hölder's inequality, Lemma 3.2.4 of [3], Lemma 2.1, (3.30), (3.35), the triangle inequality, and inverse estimates to deduce that

$$\begin{aligned}h_T^{-1/p}\|R\|_{L^q(\gamma)} \lesssim & \mathcal{G}_1\|e\|_{L^q\tilde{\omega_\gamma}} + h_T^{-1}\|\mathcal{G}\|_{L^\infty(\omega_\gamma)}\|(\mathbf{P} - \mathbf{A}_h^\ell)\nabla_\Gamma u_h^\ell\|_{L^q(\tilde{\omega_\gamma})} \\ & + \|\bar{r} - r\|_{L^q(\omega_\gamma)} + \|R - \bar{R}\|_{L^q(\gamma)}.\end{aligned}$$

The result follows after multiplying this inequality by h_T^2, equation (3.35) by h_T^2, substituting $\mathcal{G}_1$ for the right hand side of (3.30), and choosing $R = \bar{R}$ and $r = \bar{f}$.

3.3 Pointwise Estimator

Now we proceed to find a pointwise a posteriori estimator for the problem (3.1). Following [28], [44] and [21] we start the proof by writing the weak form of the problem using the Green's function as the auxiliary function.

3.3.1 Regularity properties of the Green's functions

We cite [19] Lemma 2.2.

Lemma 3.3.1 *There exists a function $G(x, y)$ (unique up to a constant) such that for all functions $u(x) \in C^2(\Gamma)$,*

$$\begin{aligned}u(x) - \frac{1}{|\Gamma|}\int_\Gamma u(x) \, d\sigma &= \int_\Gamma G(x, y)(-\triangle_\Gamma u(y)) \, d\sigma \\ &= \int_\Gamma \nabla_{\Gamma,y} G(x, y)\nabla_{\Gamma,y} u(y) \, d\sigma.\end{aligned} \quad (3.36)$$

Let $\alpha(x, y)$ be the surface distance between $x, y \in \Gamma$, and let d denote the dimension of

Γ. *Further assume that* $\alpha(x,y) < 1$. *Then (c.f. [19] Lemma 2.2, [5] Theorem 4.17)*

$$|G(x,y)| \lesssim \begin{cases} \ln\left(\frac{C}{\alpha(x,y)}\right) \text{ for } d=2, \\ \alpha(x,y)^{2-d}\ d>2. \end{cases} \tag{3.37}$$

Let $|\gamma+\beta|>0$ *where* γ,β *are multiindices. Then*

$$|D^{\gamma}_{\Gamma,y} D^{\beta}_{\Gamma,x} G(x,y)| \lesssim \alpha(x,y)^{2-d-|\gamma+\beta|}. \tag{3.38}$$

Lemma 3.3.2 *Let* $d \geq 2$ *denote the dimension of the surface* Γ. *Then*

$$G(x,y) \in W^1_p(\Gamma), \text{ where } p < \frac{d}{d-1}.$$

Proof By (3.38) we have $|G|^p_{W^1_p(\Gamma)} = \int_\Gamma |\nabla G|^p\, d\sigma \lesssim \int_\Gamma |\alpha(x,y)^{1-d}|^p\, d\sigma$. ∇G is bounded uniformly away from the singularity at $y=x$, so we analyze what happens in a y-neighborhood U of x. There is a local isomorphism χ that maps U to a disk D contained in a plane of dimension d embedded in $\mathbb{R}^{d+1}$. We let μ denote the Jacobian of the transformation $\chi : U \to D$. Then

$$|G|^p_{W^1_p(U)} \lesssim \|\mu\|_{L^\infty(D)} \int_D |r^{(1-d)p}|\ d\sigma_D,$$

where $r := |\chi(x) - \chi(y)|$, $y \subset U$. By a linear scaling we can choose χ such that $r_D = r_U$, where r_D and r_U represent the radii of D and U respectively. Then we use polar coordinates to get:

$$|G|^p_{W^1_p(U)} \lesssim \|\mu\|_{L^\infty(D)} \int_{S^d} \int_0^{r_D} r^{p(1-d)} r^{d-1}\ dr\ dS^d. \tag{3.39}$$

The last integral is finite whenever $p(1-d)+d-1 > -1$ i.e. $p < \frac{d}{d-1}$. This completes the proof.

Corollary 3.3.3 *Let* p *satisfy* $p < \frac{d}{d-1}$. *Then there is a constant,* $C(p,d)$, *depending on* p *and* d *such that* $|G|_{W^1_p(U)} \lesssim C(p,d)$ *and* $C(p,d) \to \infty^+$ *as* $p \to \left(\frac{d}{d-1}\right)^-$.

Proof From (3.39) we get

$$|G|_{W^1_p(U)} \lesssim \frac{1}{[d-p(d-1)]^{1/p}} r_D^{1-d+d/p}, \tag{3.40}$$

where $r_D > 0$ is a fixed constant and clearly $C(p,d) := \left(\frac{1}{d-p(d-1)}\right)^{1/p} \to \infty^+$ as $p \to \left(\frac{d}{d-1}\right)^-$.

Lemma 3.3.4 *Let x_0 be the singularity of the Green's function and let U be a neighborhood of x_0 such that there is a constant c_1 for which the disk of radius c_1 centered at x_0 is contained in the interior of U (i.e $B_{c_1}(x_0) \subset \mathring{U}$). Then*

$$|G|_{W_1^2(\Gamma\setminus U)} \lesssim 1 + \ln\left(\frac{1}{c_1}\right). \tag{3.41}$$

Proof Let c_2 denote the diameter of Γ. By equation (3.38),

$$|G|_{W_1^2(\Gamma\setminus U)} \lesssim \int_{c_1}^{c_2} r^{-1}\, dr \lesssim 1 + \ln\left(\frac{1}{c_1}\right).$$

3.3.2 Estimator

We are ready now to state and prove the main result. Define:

$$e := u(x) - u_h^\ell(x) + \frac{1}{|\Gamma|}\int_\Gamma u_h^\ell(x)\, d\sigma. \tag{3.42}$$

Theorem 3.3.5 *Let $u(x)$ be the solution to the Laplace-Beltrami equation* (3.1)*, let $\underline{h} = \min_{\{T\in\mathcal{T}\}}\{h_T\}$, $d \geq 2$, $q_1 > \frac{d}{2}$, $q_2 > d$, $q_3 > d-1$, and $q_4 > \frac{d}{2}$. Let $\theta(T)$ be as in* (3.9) *and define $\hat{\theta}_\infty(T) := \theta_\infty(T) + \|\frac{1}{\mu_h}\|_{L^\infty(T)}\|\mathbf{I} - d\mathbf{H}\|_{L^\infty(T)}$ and similarly for $\hat{\theta}_\infty(\omega_T)$. Then for $x \in \Gamma$, there holds*

$$\begin{aligned} |e(x)| \lesssim \max_{T\in\mathcal{T}}\Big\{\hat{\theta}_\infty(\omega_T)(1+|\ln \underline{h}|)\Big(h_T^{2-d/q_1}\|\mu_h f^\ell + \triangle_{\Gamma_h} u_h\|_{L^{q_1}(T)} \\ + h_T^{1-(d-1)/q_3}\|[\![\nabla_{\Gamma_h} u_h]\!]\|_{L^{q_3}(\partial\mathcal{T})}\Big)\Big\} + \|(\mathbf{P} - \mathbf{A}_h^\ell)\nabla_\Gamma u_h^\ell\|_{L^{q_2}(\Gamma)} \\ + \tilde{C}_{q_4}\|\mu_h f^\ell - f_h\|_{L^{q_4}(\Gamma_h)}. \end{aligned} \tag{3.43}$$

The constant in "$\lesssim$" depends on shape regularity properties of $\mathcal{T}$ and on properties of Γ via the Green's function G, and blows up as $q_2 \to d^+$, $q_3 \to (d-1)^+$ or $q_1, q_4 \to \frac{d}{2}^+$ respectively, and $\tilde{C}_{q_4}$ depends on q_4, $\|\frac{1}{\mu_h}\|_{L^\infty(\Gamma)}$, and $\|\mathbf{P} - d\mathbf{H}\|_{L^\infty(\Gamma)}$.

Remark In (3.43) we use Sobolev embeddings in order to define elementwise residuals measured in L_q norms for $q < \infty$. This has two advantages. It allows us to admit data f not in L^∞, and to measure the geometric term $\|(\mathbf{P} - \mathbf{A}_h^\ell)\nabla_\Gamma u_h^\ell\|_{L^{q_2}(\Gamma)}$ in a weaker norm in the event $u \notin W_\infty^1(\Gamma)$. Our methodology yields no advantage in the jump residual terms for constant-coefficient operators, but does in the case of nonconstant diffusion coefficients. In our numerical experiments we simply take $q_i = \infty$ for all i.

Inequality (3.43) is similar to the results for flat domains $\Omega \in \mathbb{R}^n$ obtained in [28], [44] and [21].

Proof We make use of equations (3.36) and (3.29) to rewrite (3.42) as

$$e(x) = \int_\Gamma \nabla_{\Gamma y} G(x,y) \nabla_\Gamma \Big(u - u_h^\ell \Big) \, d\sigma. \tag{3.44}$$

Let $G^\ell(x,y) = G(x,a(y))$ for $y \in \Gamma_h$ and let $G_h = I_h G^\ell$. The residual equation (3.14) yields

$$\begin{aligned} e(x) &= \int_\Gamma \nabla_{\Gamma y} G \nabla_\Gamma \Big(u(y) - u_h^\ell(y) \Big) \, d\sigma \\ &= \int_{\Gamma_h} r(G^\ell - G_h) \, d\sigma_h - \int_\Gamma [(\mathbf{P} - \mathbf{A}_h^\ell) \nabla_\Gamma u_h^\ell] \cdot \nabla_\Gamma G \, d\sigma \\ &\quad - \frac{1}{2} \sum_{T \in \mathcal{T}} \int_{\partial T} R(G^\ell - G_h) \, ds + \int_{\Gamma_h} (\mu_h f^\ell - f_h) G_h \, d\sigma_h. \end{aligned} \tag{3.45}$$

For $j = \{1,2,3,4\}$ let $p_j, q_j, s_j, t_j \geq 1$ be such that $p_1, p_4 < \frac{d}{d-2}$, $p_2 < \frac{d}{d-1}$, $p_3 < \frac{d-1}{d-2}$, $\frac{1}{p_j} + \frac{1}{q_j} = 1$, and $\frac{1}{s_j} + \frac{1}{t_j} = 1$. We first recall (3.29) and apply Hölder's inequality to (3.45). Then we apply (2.32) while choosing $m = 1$ or $m = 2$ according to the criteria explained below. For $m = 1$ we pick $\frac{dp_j}{d+p_j} = s_j < \frac{d}{d-1}$, satisfying Lemma 2.4.6. For $m = 2$ we pick $s_j = 1$. This yields

$$\begin{aligned} |e(x)| \lesssim \sum_{T \in \mathcal{T}} \Big\{ & \|r\|_{L^{q_1}(T)} \|G^\ell - G_h\|_{L^{p_1}(T)} \\ & + \|(\mathbf{P} - \mathbf{A}_h^\ell) \nabla_\Gamma u_h^\ell\|_{L^{q_2}(a(T))} \|\nabla_\Gamma G\|_{L^{p_2}(a(T))} \\ & + \|R\|_{L^{q_3}(\partial T)} \|G^\ell - G_h\|_{L^{p_3}(\partial T)} \\ & + \|\mu_h f^\ell - f_h\|_{L^{q_4}(T)} \|G_h\|_{L^{p_4}(T)} \Big\}, \end{aligned}$$

$$\begin{aligned} |e(x)| \lesssim \sum_{T \in \mathcal{T}} \Big\{ & \|r\|_{L^{q_1}(T)} h_T^{m - d/s_1 + d/p_1} \sum_{T_i \in \omega_T} |G^\ell|_{W_{s_1}^m(T_i)} \\ & + \|(\mathbf{P} - \mathbf{A}_h^\ell) \nabla_\Gamma u_h^\ell\|_{L^{q_2}(a(T))} \|\nabla_\Gamma G\|_{L^{p_2}(a(T))} \\ & + \|R\|_{L^{q_3}(\partial T)} h_T^{m - d/s_3 + (d-1)/p_3} \sum_{T_i \in \omega_T} |G^\ell|_{W_{s_3}^m(T_i)} \\ & + \|\mu_h f^\ell - f_h\|_{L^{q_4}(T)} \|G_h\|_{L^{p_4}(T)} \Big\}. \end{aligned} \tag{3.46}$$

Let $T_0 = \{T \in \mathcal{T}_h \colon x \subset \overline{T}\}$. Let also $\omega_T' = \{T' \in \mathcal{T} : \overline{T'} \cap \overline{\omega_T} \neq \emptyset\}$. Subsequently we split the terms involving $|G^\ell|_{W_{s_j}^m(T_i)}$, $T_i \in \omega_T$ in two sets covering Γ_h. If $T \in \omega_{T_0}'$ we choose $m = 1$ and $m = 2$ if $T \in \mathcal{T} \setminus \omega_{T_0}'$. In the first case we pick $s_1 = \frac{dp_1}{d+p_1}$ so $m - \frac{d}{s_1} + \frac{d}{p_1} = 0$, and in the latter case we pick $s_1 = 1$ so $m - \frac{d}{s_1} + \frac{d}{p_1} = 2 - d + \frac{d}{p_1}$ and observe that $\sum_{T \in \mathcal{T} \setminus \omega_{T_0}'} \Big(\sum_{T_i \in \omega_T} |G^\ell|_{W_1^2(T_i)} \Big) \leq |G^\ell|_{W_1^2(\Gamma_h \setminus \omega_{T_0})}$. Then it follows from

(3.40) with $r_D = h_T$ and $p_1 < \frac{d}{d-2}$, (3.41) with $c_1 = h_T$ and the same choice of p_1 that

$$\begin{aligned}&\sum_{T\in\omega'_{T_0}} \|r\|_{L^{q_1}(T)} h_T^{1-d+d/p_1} \sum_{T_i\in\omega_T} |G^\ell|_{W^1_{s_1}(T_i)}\\ &\qquad\lesssim \|\frac{1}{\mu_h}\|_{L^\infty(T)} \|\mathbf{I} - d\mathbf{H}\|_{L^\infty(T)} \max_{T\in\omega'_{T_0}} \left\{ \|r\|_{L^{q_1}(T)} h_T^{2-d/q_1} \right\}\end{aligned} \tag{3.47}$$

and

$$\begin{aligned}&\sum_{T\in\mathcal{T}\setminus\omega'_{T_0}} \|r\|_{L^{q_1}(T)} h_T^{2-d+d/p_1} \sum_{T_i\in\omega_T} |G^\ell|_{W^2_1(T_i)}\\ &\qquad\lesssim \hat{\theta}_\infty(\omega_T) \max_{T\in\mathcal{T}\setminus\omega'_{T_0}} \left\{ \|r\|_{L^{q_1}(T)} h_T^{2-d/q_1} \right\} (1 + |\ln \underline{h}|).\end{aligned} \tag{3.48}$$

The terms $\|\mathbf{I} - d\mathbf{H}\|_{L^\infty(T)}$ and $\hat{\theta}_\infty(\omega_T)$ come from the chain rule and Lemma 3.1.1. Then by a similar argument with $s_3 = 1$ when $m = 2$ and $s_3 = \frac{dp_3}{d+p_3}$ when $m = 1$ we get

$$\begin{aligned}&\sum_{T\in\omega'_{T_0}} \|R\|_{L^{q_3}(\partial T)} h_T^{1-d+(d-1)/p_3} \sum_{T_i\in\omega_T} |G^\ell|_{W^1_{s_3}(T_i)}\\ &\qquad\lesssim \left\| \frac{1}{\mu_h} \right\|_{L^\infty(T)} \|\mathbf{I} - d\mathbf{H}\|_{L^\infty(T)} \max_{T\in\omega'_{T_0}} \left\{ \|R\|_{L^q(\partial T)} h_T^{1-(d-1)/q_3} \right\},\end{aligned} \tag{3.49}$$

$$\begin{aligned}&\sum_{T\in\mathcal{T}\setminus\omega_{T_0}} \|R\|_{L^{q_3}(\partial T)} h_T^{2-d+(d-1)/p_3} \sum_{T_i\in\omega_T} |G^\ell|_{W^2_1(T_i)}\\ &\qquad\lesssim \hat{\theta}_\infty(\omega_T) \max_{T\in\mathcal{T}\setminus\omega'_{T_0}} \left\{ \|R\|_{L^{q_3}(\partial T)} h_T^{1-(d-1)/q_3} \right\} (1 + |\ln \underline{h}|).\end{aligned} \tag{3.50}$$

Pick $s_4 = \frac{dp_4}{d+p_4}$. Then an inverse estimate $\|G_h\|_{L^{p_4}} \lesssim h_T^{-d/s_4+d/p_4} \|G_h\|_{L^{s_4}(T)}$ and (2.33) yield

$$\begin{aligned}&\sum_{T\in\mathcal{T}} \|\mu_h f^\ell - f_h\|_{L^{q_4}(T)} \|G_h\|_{L^{p_4}(T)}\\ &\quad\le \sum_{T\in\mathcal{T}} \|\mu_h f^\ell - f_h\|_{L^{q_4}(T)} h_T^{-d/s_4+d/p_4} \|G_h\|_{L^{s_4}(T)}\\ &\quad\le \sum_{T\in\mathcal{T}} \|\mu_h f^\ell - f_h\|_{L^{q_4}(T)} \sum_{K\in\omega_T} h_T^{-d/s_4+d/p_4} \big\{ \|G^\ell\|_{L^{s_4}}(T)\\ &\qquad + h_T \|\nabla G^\ell\|_{L^{s_4}(T)} \big\}.\end{aligned} \tag{3.51}$$

From Hölder's inequality follows $h_T^{-d/s_4+d/p_4} \|G^\ell\|_{L^{s_4}}(T) \le \|G^\ell\|_{L^p_4}$. $1 - \frac{d}{s_4} + \frac{d}{p_4} = 0$ by our choice of s_4, and since $s_4 \le p_4$ it follows that $(\sum_{T\in\mathcal{T}} \|\nabla_{\Gamma_h} G^\ell\|^{p_4}_{L^{s_4}(\omega_T)})^{1/p_4} \le$

$(\sum_{T\in\mathcal{T}}\|\nabla_{\Gamma_h}G^\ell\|^{s_4}_{L^{s_4}(\omega_T)})^{1/s_4}$. Thus

$$\begin{aligned}
&\sum_{T\in\mathcal{T}}\|\mu_h f^\ell - f_h\|_{L^{q_4}(T)}\|G_h\|_{L^{p_4}(T)}\\
&\quad\le\sum_{T\in\mathcal{T}}\|\mu_h f^\ell - f_h\|_{L^{q_4}(T)}\sum_{K\in\omega_T}\left\{\|G^\ell\|_{L^{p_4}}(T)+\|\nabla_{\Gamma_h}G^\ell\|_{L^{s_4}(T)}\right\}\\
&\quad\le C_{G,q_4}\Big(\sum_{T\in\mathcal{T}}[(C_{p_4}(\omega_T)\\
&\qquad + C_{s_4}(\omega_T)\|\mathbf{P}-d\mathbf{H}\|_{L^\infty(\omega_T)})\|\mu_h f^\ell - f_h\|_{L^{q_4}(T)}]^{q4}\Big)^{1/q_4}.
\end{aligned}\tag{3.52}$$

Here $C_{G,q_4}=\|G\|_{L_{p_4}(\Gamma)}+\|\nabla_\Gamma G\|_{L_{S_4}(\Gamma)}$. Because $s_4=\frac{dp_4}{d+p_4}\to\frac{d}{d-1}^-$ as $p_4\to\frac{d}{d-2}^-$ we see that C_{G,q_4} blows up as $p_4\to\frac{d}{d-2}^-$ (i.e. $q_4\to\frac{d}{2}^+$). Thus

$$\sum_{T\in\mathcal{T}}\|\mu_h f^\ell - f_h\|_{L^{q_4}(T)}\|G_h\|_{L^{p_4}(T)}\lesssim C_{G,q_4}\tilde{C}_{q_4}\|\mu_h f^\ell - f_h\|_{L^{q_4}(\Gamma_h)}.\tag{3.53}$$

Similarly

$$\sum_{T\in\mathcal{T}}\|(\mathbf{P}-\mathbf{A}_h^\ell)\nabla_\Gamma u_h^\ell\|_{L^{q_2}(a(T))}\|\nabla_\Gamma G\|_{L^{p_2}(a(T))}\lesssim C_{q_2}\|(\mathbf{P}-\mathbf{A}_h^\ell)\nabla_\Gamma u_h^\ell\|_{L^{q_2}(\Gamma)},\tag{3.54}$$

where Corollary 3.3.3 gives that $C_{q_2}\to\infty$ as $p_2=\to\frac{d}{d-1}^-\iff q_2\to d^+$. Combining equations (3.46), (3.47), (3.48), (3.49), (3.50), (3.53) and (3.54) to get (3.43) finishes the proof of the Theorem.

3.3.3 Efficiency

Lemma 3.2.5 gives that the residual parts of the error indicator are bounded by the L^∞ norm of the error plus some higher order geometric terms when $q_1=q_3=\infty$.

$$\begin{aligned}
\mathcal{R}:=&h_T^2\|\mu_h f^\ell+\triangle_{\Gamma_h}u_h\|_{L^\infty(T)}+h_T\|[\![\nabla_{\Gamma_h}u_h]\!]\|_{L^\infty(\partial T)}\\
&\lesssim\|e\|_{L^\infty(\tilde{\omega}_T)}(\|\mathcal{G}\|_{L^\infty(\omega_T)}+h_T\|D\mathcal{G}\|_{L^\infty(\omega_T)})\\
&\quad+h_T\|\mathcal{G}\|_{L^\infty(\omega_T)}\|(\mathbf{P}-\mathbf{A}_h^\ell)\nabla_\Gamma u_h^\ell\|_{L^\infty(\tilde{\omega}_T)}+h_T^2\|\mu_h(\bar{f}-f)\|_{L^\infty(\tilde{\omega}_T)}.
\end{aligned}\tag{3.55}$$

Similar estimates follows easily from Hölder's inequality for other allowable choices of q_1, q_3.

3.4 Numerical Experiments

In this section we use our a posteriori estimates to implement an Adaptive Surface Finite Element Method (ASFEM). We use a maximum marking strategy with threshold 0.25, that is, we mark T for refinement if $\eta(T)\ge 0.25\max_{T'\in\mathcal{T}}\eta(T')$. We tuned our error indicator using empirical constant factors multiplying the residual components in order to ensure that estimators and errors had similar magnitudes. For the L^2

case the factor chosen was 0.001 and 0.01 for the pointwise case. The error indicator for the pointwise estimator is based on (3.43), where we choose all $q_i = \infty$ for $i = \{1, 2, 3, 4\}$. We used iFEM [14] as a platform for our numerical experiments.

We first consider the torus obtained by rotating the circle $(x-4)^2 + z^2 = 3.9^2$ about the z-axis. We take $u = x$ and show the adaptive results for the L^2 estimator. This torus has large curvature inside of its "doughnut hole", so we expect geometric components of the estimator to be important. In the right chart in Figure 3-1 the

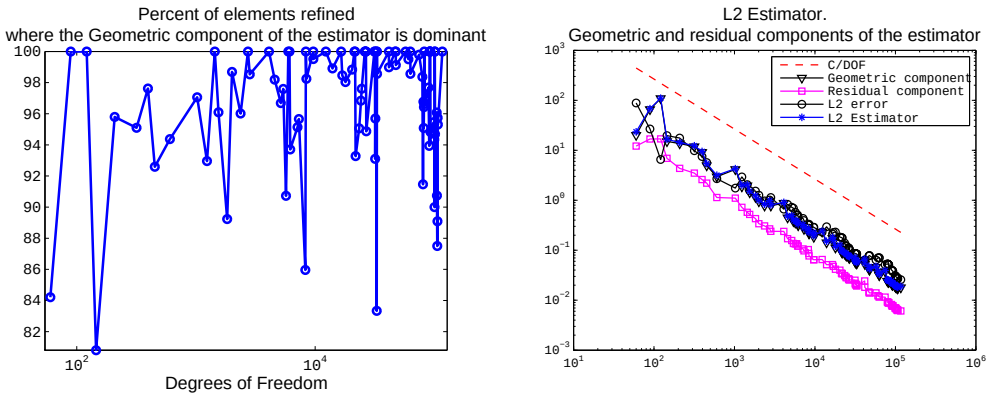

Figure 3-1: Results for ASFEM solving $-\triangle_\Gamma u = f$ with Γ a torus having major radius 4 and minor radius 3.9 and $u = x$. *Left:* Percent of elements marked for refinement whose geometric component of the estimator is higher than the residual one. *Right:* Evolution of the L^2 error, estimator, and the geometric and residual components of the estimator.

geometric part of the estimator and the overall estimator practically overlap. The residual part is about one order of magnitude smaller than the geometric part. Both the geometric and residual components appear to decrease at optimal rate DOF^{-1}. In the left figure we observe that the majority of elements refined have a dominant geometric component. Thus in this example the refinement is mostly being driven by the geometric component of the estimator. Note however that which component dominates also depends on the choice of constants multiplying the estimator components.

We next take Γ as above but $u = \exp\left(\frac{1}{62.6975 - x^2}\right)$. The residual component of the estimator is more important than when $u = x$ above (left chart in Figure 3-2), which is expected because u has an exponential peak on the outer radius of the torus were the curvatures and thus geometric error effects are small. In the right chart of Figure 3-2 we observed unexpected oscillations in the geometric component of the L^2 estimator and to some extent also the error even on fine meshes. This initially seems counterintuitive since refinement usually yields nearly monotonically decreasing estimators. After a careful analysis we observed that although the initial mesh is nearly transverse to Γ, some of the intermediate meshes are not, as illustrated in Figure 3-3. We identify this phenomena as the cause of the oscillations. In particular, the quality of the approximation of ν by ν_h may be worse on a finer mesh, affecting all the quantities whose calculation depends on it. These include the Jacobian

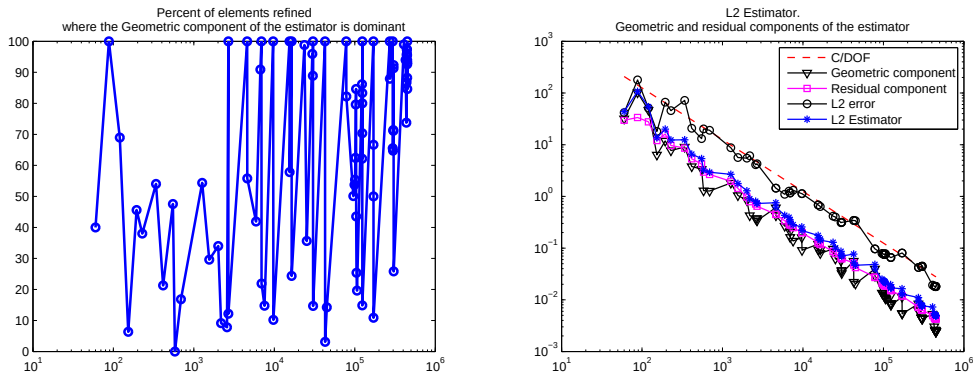

Figure 3-2: Results for ASFEM on a torus with major and minor radii 4 and 3.9 and $u = \exp\left(\frac{1}{62.6975-x^2}\right)$. In the left plot we graph the percent of elements refined whose geometric component of the estimator is higher than the residual one. In the right plot we show the evolution of the L^2 error, residual and its components.

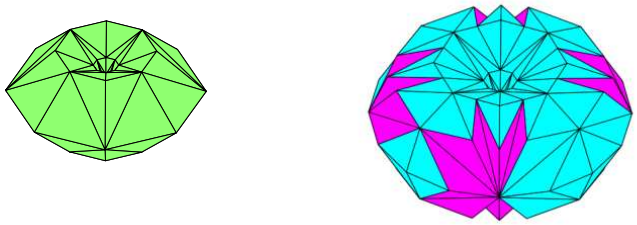

Figure 3-3: *Left:* The initial transverse triangulation. *Right:* An intermediate triangulation. The right mesh contains darkly-shaded non-transverse elements that cause "kinks" in Γ_h. These were marked for refinement by ASFEM due to large geometric estimators.

$\mu_h = \nu \cdot \nu_h(1 - d(x)\kappa_1(x))(1 - d(x)\kappa_2(x))$ [20], $\mathbf{A}_h$ defined in (2.12) and $\mathbf{P}_h$. When we performed uniform refinement of the mesh, the oscillation and non-transverse intermediate meshes were not observed. Even for adaptive refinement asymptotic convergence rates are not affected by these geometric artifacts, and a quasi-monotone decrease of the geometric error may still be expected [8].

For the second example we use the torus obtained by rotating the circle $(x - 4)^2 + z^2 = 1$ over the $z-$axis and choose $u = \exp\left(\frac{1}{25.2875-x^2}\right)$. The solution has an exponential peak around the points $(\pm 5, 0, 0)$. We use ASFEM based on the L^2 and pointwise error estimators. All components of the estimator converge with optimal rate DOF^{-1} (the error plots are standard and thus not pictured). In Figure 3-4 we present meshes obtained by our L^2 and pointwise ASFEMs showing more refinement near the points $(\pm 1, 0, 0)$. This is expected since the solution has exponential peaks there and the geometric quantities $\mathbf{H}, \mathbf{H}_{x_i}$ are relatively small on Γ. The pointwise estimator gives a higher density of refinement near $(\pm 1, 0, 0)$ than the L^2 estimator, as is expected since the maximum norm is stronger.

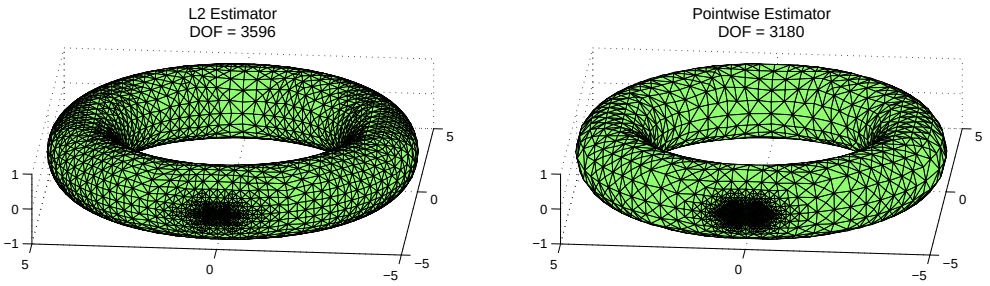

Figure 3-4: Intermediate meshes obtained by adaptive refinement based on L^2 (left) and pointwise (right) estimators.

For the final example we apply our estimator to a spherical wedge $\Gamma := \{(\rho, \phi, \theta) : \rho = 1, 0 \leq \phi \leq \pi, 0 \leq \theta \leq \frac{5\pi}{3}\}$ (Figure 3-5). We chose $u = \sin(\lambda\theta)\sin(\phi)^\lambda$. Our theory does not apply to this example since Γ is not closed. Γ has a re-entrant corner and is thus a surface counterpart of a nonconvex polygonal (Euclidean) domain. Our proof for the L^2 a posteriori estimator relies on H^2 regularity, which does not hold on nonconvex polygonal domains or for Γ. Thus we expect the L^2 estimator to be unreliable as on nonconvex polyhedron; cf. [40, 62]. This is confirmed in the left plot of Figure 3-5, which shows that the L^2 error decreases at a slower rate than our estimator. The jump term $\|[\![\nabla_{\Gamma_h} u_h]\!]\|_{L^2(\partial T)} h_T^{3/2} \theta_2(\omega_T))$ dominates the estimator asymptotically, so we compare it to the L^2 error. This corroborates that the L^2 estimator is not reliable. On the other hand we expect the pointwise estimator to be reliable as on nonconvex

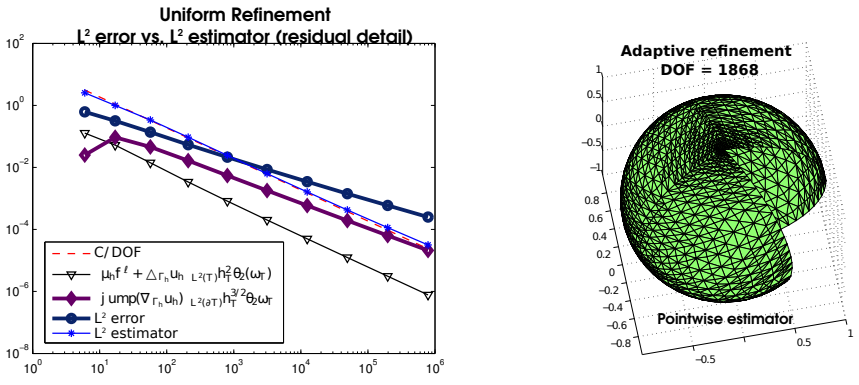

Figure 3-5: In the left plot we show the L^2 error decrease versus the residual part of the L^2 estimator. On the right plot we show a mesh obtained by adaptive refinement based on our pointwise estimator

polyhedra [44, 21] and the corresponding ASFEM to yield optimal mesh refinement.

This is confirmed in Figure 3-6, which shows that our estimator is reliable under both uniform and adaptive refinement and that the pointwise ASFEM achieves optimal convergence.

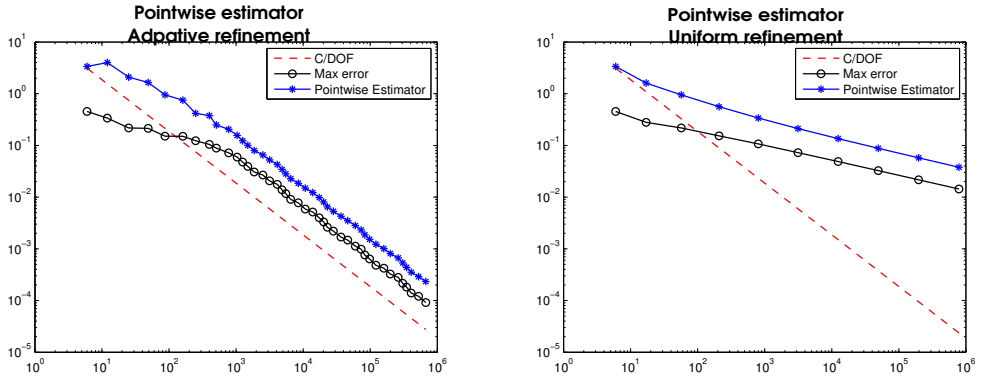

Figure 3-6: We show the error and estimator plots for the pointwise estimator using adaptive refinement and uniform refinement

3.4.1 Remark on the importance of the geometric terms in the numerical tests

We have discussed in the previous section that the additive geometric component $\|(\mathbf{P}-\mathbf{A}_h^\ell)\nabla_\Gamma u_h^\ell\|$ of our L^2 and pointwise estimates can dominate the adaptive refinement process. Besides the geometric additive part our error estimates also include multiplicative geometric terms[1] that arise naturally when moving between Γ and Γ_h. Exact calculation of these multiplicative components is not practical, and numerical estimation can be expensive. In particular we analyse the effect of replacing $\theta(\cdot)$ by a constant equal to one. We recall that in (3.9) we define

$$\theta_p(T) := \left\| \frac{1}{\mu_h} \right\|^p_{L^\infty(K)} \Big(\|\mathbf{P}_h[\mathbf{I}-d\mathbf{H}]\|^2_{L^\infty(a(T))} + \|\mathbf{P_h H}\|_{L^\infty(a(K))} \|\vec{\nu}-(\vec{\nu}\cdot\vec{\nu}_h)\vec{\nu}_h\|_{L^\infty(a(T))} + \max_{i=1,2,3} \|d\mathbf{P}_h\mathbf{H}_{x_i}\|_{L^\infty(a(T))} \Big).$$

We note that $\left|1-\|\mathbf{P}_h[\mathbf{I}-d\mathbf{H}]\|^2_{L^\infty(a(T))}\right| = \mathcal{O}(h_T^2)$, $\|\vec{\nu}-(\vec{\nu}\cdot\vec{\nu}_h)\vec{\nu_h}\|_{L^\infty(a(T))} = \mathcal{O}(h_T)$, and $\max_{i=1,2,3}\|d\mathbf{P}_h\mathbf{H}_{x_i}\|_{L^\infty(a(T))} = \mathcal{O}(h_T^2)$. For fine enough meshes $\mu_h \approx 1$, thus $|1-\theta_p(T)| = \mathcal{O}(h_T)$.

Next show the results for a numeric test where we take $u = \exp\left(\frac{1}{62.6975-x^2}\right)$ to the solution of (3.1). Here Γ is the torus with parametric equation

$$\Gamma = \begin{cases} x(\psi,\phi) = [4+3.9\cos(\psi)]\cos(\phi), \\ y(\psi,\phi) = [4+3.9\cos(\psi)]\sin(\phi), \\ z(\psi) = 3.9\sin(\psi), \\ \psi,\ \phi \in [0,\pi]. \end{cases} \tag{3.56}$$

[1] See (3.9) and their pointwise counterparts defined on Theorem 3.3.5.

Figure 3-7 shows that for fine enough meshes $|1-\theta_2(T)| = \mathcal{O}(h_T) \sim \frac{C}{\sqrt{DOF}}$. Initially

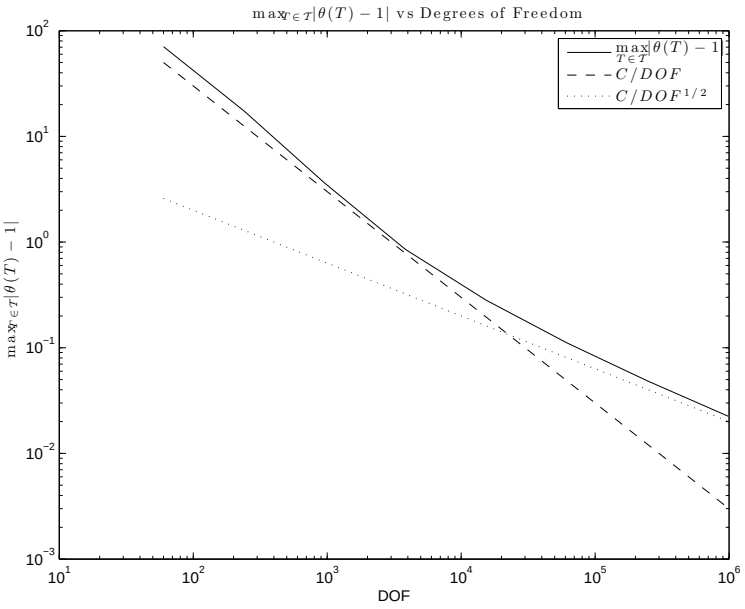

Figure 3-7: Evolution of $|\theta(T)-1|$

the expression is dominated by the term $\left|1-\|\mathbf{P}_h[\mathbf{I}-d\mathbf{H}]\|^2_{L^\infty(a(T))}\right|$, thus $|1-\theta_2(T)|$ initially decreases with order $\mathcal{O}(h_T^2) \sim \frac{C}{DOF}$.

A important question is how much is the performance of the adaptive algorithm affected when we set $\theta_2(T) = 1$. A comparison between the results obtained when $\theta_2(T)$ is calculated versus set to be constant are shown in Figure 3-8 The multiplicative term θ_2 only affects the residual component of the error estimator. In Figure 3-8 we show that asymptotically the residual part of the estimator behaves the same when θ_2 is set to be constant versus when it is computed. Similar results were obtained when the solution of (3.1) is taken to be $u = x$.

Preliminary tests suggest that we can safely set $\theta_2(T) = 1$ and the accuracy of the estimator would not be negatively affected. A more rigorous analysis is desirable to find conditions when this assertion holds. The advantages of avoiding extra, possibly unnecessary, computation are obvious. They will be particularly important in the next chapter when the need of implementing faster algorithms is more critical.

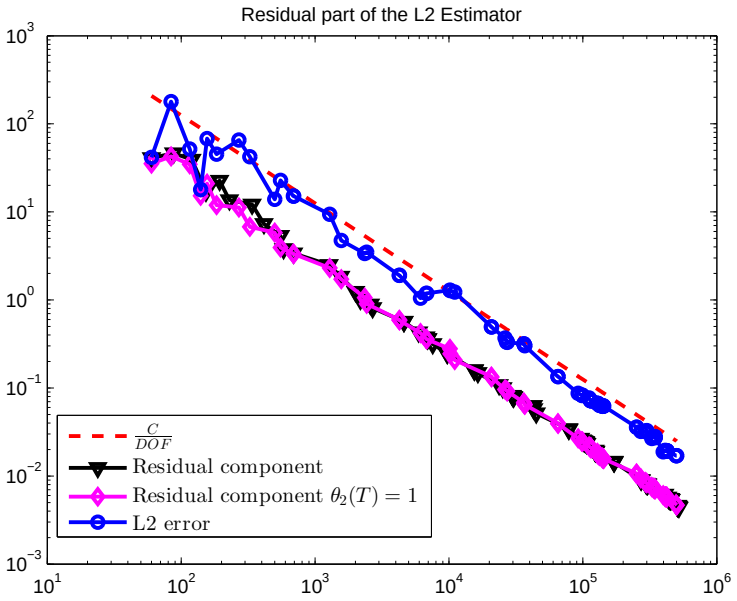

Figure 3-8: Comparison between the estimator results when $\theta_2(T)$ is computed versus set to be constant

THIS PAGE INTENTIONALLY LEFT BLANK

Chapter 4

A posteriori estimate for surface parabolic equations

In this chapter we adapt the results obtained in sections 3.2 and 3.3 to obtain an a posteriori error estimator for the heat equation on a fixed surface. The technique that we use is similar to the one proposed for flat surfaces in [41]. For future work we are interested in transitioning to evolving surface finite element methods (ESFEM) [27], [25]. The stationary surface problem introduces some of the features that we need to consider for the evolving surface case. For example, an efficient numerical implementation solving the heat equation in stationary or evolving surfaces would require mesh coarsening. Mesh coarsening helps to keep a manageable size of the computational problem [50], [43]. Time stepping is also a common feature of problems in both stationary and evolving surfaces.

Another practical consideration is that computational cost of time dependent problems is considerably larger than the one for time independent ones. Hence, for implementation, it becomes important to use numerical schemes that require fewer time steps and fewer floating point operations. Adaptivity may require larger running times; that is why many time dependent applications don't use adaptive refinement. However adaptivity offers the advantage of greater accuracy with less memory. Some work discussing how to implement adaptive refinement on moving meshes can be found in [13] and [35].

In order to reduce the computational and theoretical overhead of our parabolic error estimates, we neglect the multiplicative geometric constants $\theta_p(\cdot)$, $C_p(\cdot)$, $\theta_\infty(\omega_k)$ and $\gamma_2(\cdot)$ defined in Section 3.2. We point out that from our numerical experiments we observed that the convergence rate of the estimator was not heavily impacted by these constants. In the other hand the additive geometric term $\|[\mathbf{P} - \mathbf{A}_h^\ell]\nabla_\Gamma u_h^\ell(t)\|_{L^2(a(T))}$ plays an important role in the convergence of the AFEM. That is why we include it in our error estimate.

4.1 Introduction

Elliptic reconstruction is a technique for proving a posteriori error estimates for parabolic equations. It was introduced for spatially semidiscrete schemes by Nochetto and Makridakis [41]. It had previously been observed that "usual" energy techniques for proving a posteriori error estimates yield suboptimal rates of convergence in the $L^\infty(0,T;L^2(\Omega))$ norm. Here Ω is the spatial domain and $[0,T]$ is the time interval.

Fully discrete versions (discretized in time and space) yielding results valid for energy norms have been given by Lakkis and Makridakis [39]. Demlow, Lakkis and Makridakis proved results for the maximum norm valid for semidiscrete and fully discrete schemes [22]. Kopteva and Linss proved a posteriori error estimates in the maximum norm for semilinear second order parabolic equations. Their estimates are valid for semidiscrete schemes and for fully discrete schemes using backward Euler

and Crank-Nicholson time discretizations [38].

4.2 Finite element approximation

In the same way as in the previous chapter we consider conformal consistent Galerkin approximation schemes, and our meshes are assumed to be conforming and shape regular. We discuss some known results for flat surfaces. Assume that Γ is a flat surface and consider the heat equation with homogeneous Dirichlet boundary conditions. Further assume that initial value conditions are such that the problem is well posed in the sense of Hadamard. For domains $\Omega \in \mathbb{R}^n$ it is known that the following a posteriori bound for the heat equation holds (cf. Theorem 3.1 of [41])

$$\begin{aligned}\max_{0\leq t\leq T} \|u(t) - u_h(t)\|_{L^2(\Omega)} \leq & \|u(0) - u_h(0)\|_{L^2(\Omega)} + \left(\int_0^T \mathcal{E}(u_{h,t}, g_{h,t}; H^{-1})^2\right)^{1/2} \\ & 2 \max_{0\leq t\leq T} \mathcal{E}(u_{h,t}, g_{h,t}; L^2).\end{aligned} \tag{4.1}$$

Here $\mathcal{E}(u_{h,t}(t), g_{h,t}, X)$ is an elliptic a posteriori estimator function depending on the finite element solution to the heat equation $u_{h,t}$, g_h, t is an "equivalent" load vector associated with the elliptic reconstruction of the heat equation, and the space $X \in \{L^2(\Omega), H^{-1}(\Omega)\}$.

In this chapter we prove an a posteriori version of (4.1) for the case when Γ is not necessarily a flat surface. For $\mathcal{E}(u_{h,t}(t), g_{h,t}, L^2)$ we use (3.10), and derive $\mathcal{E}(u_{h,t}(t), g_{h,t}, H^{-1})$ repeating the argument used to pove (3.10) with minor modifications. In order to simplify notation we write $\mathcal{E}_{L^2}$ and $\mathcal{E}_{H^{-1}}$ instead of $\mathcal{E}(u_{h,t}(t), g_{h,t}, L^2)$ and $\mathcal{E}(u_{h,t}(t), g_{h,t}, H^{-1})$ respectively.

4.2.1 Model problem

We consider the surface heat equation over a surface with smooth boundary.

$$\begin{aligned} u_t - \triangle_\Gamma u &= f \text{ in } \Gamma \times [0,T], \\ u(\cdot, 0) &= u_0(\cdot) \text{ in } \Gamma, \\ u &= 0 \text{ on } \partial\Gamma \times [0,T]. \end{aligned} \tag{4.2}$$

Here $\triangle_\Gamma$ is the Laplace-Beltrami operator defined in (2.8) and (2.9).

The results proved in Chapter 3 were obtained assuming that $\Gamma = \emptyset$. In this chapter we assume that $\partial\Gamma$ is smooth. The proof for both cases is basically the same. Since we are using Dirichlet boundary conditions the boundary terms cancel the same way they did when we assumed empty boundary. The difference is that we do not need to assume that $\int_\Gamma u(t)\ \mathrm{d}\sigma = 0$ nor $\int_\Gamma f\ \mathrm{d}\sigma = 0$ to guarantee existence and uniqueness of the solution.

4.2.2 Bilinear forms

We define the continuous bilinear form $a(\cdot,\cdot)$ by

$$a(u,v) := \int_\Gamma \nabla_\Gamma u \cdot \nabla_\Gamma v \ \mathrm{d}\sigma, \tag{4.3}$$

and discrete bilinear form $a_h(\cdot,\cdot)$ by

$$a_h(u_h,v_h) := \int_{\Gamma_h} \nabla_{\Gamma_h} u_h \cdot \nabla_{\Gamma_h} v_h \ \mathrm{d}\sigma_h. \tag{4.4}$$

We take $V = H_0^1$; and equip it with the induced norm

$$\|v\|_{H^1} := a(v,v)^{1/2}. \tag{4.5}$$

We use $(\cdot,\cdot)_h$ to denote the L^2 discrete inner product

$$(u_h,v_h)_h = \int_{\Gamma_h} u_h v_h \ \mathrm{d}\sigma_h. \tag{4.6}$$

4.2.3 Discrete Elliptic operator A_h

In this section we let the finite element space S_h to be either piecewise linear or piecewise quadratic functions. We let u_h, be the Finite Element approximation of u solving the equation

$$(u_{h,t},\chi)_h + a_h(u_h,\chi) = (f_h,\chi)_h \ \forall\ \chi \in S_h. \tag{4.7}$$

Here $u_h(\cdot,t) \in S_h$ for each t, and u_h is continuously differentiable in time, and f_h is an approximation to f. For convenience we choose $f_h \in S_h$. We then define the discrete Laplace-Beltrami operator A_h by

$$(A_h u_h, v_h)_h = a_h(u_h,v_h), \text{ for } v_h \in S_h, \tag{4.8}$$

A_h then satisfies pointwise

$$u_{h,t} + A_h u_h = f_h. \tag{4.9}$$

4.2.4 Matrix formulation

We start by writing u_h as a linear combination of the basis elements of S_h:

$$u_h = \sum_{i=1}^{N} U_i(t)\phi_i, \tag{4.10}$$

where the coefficients U_i are a function of time and the basis elements $\{\phi_i\}_{i=1}^N$ depend only on the spatial coordinates.

Using the same idea as in (1.16) we write

$$\begin{aligned}\mathbf{BU}_t + \mathbf{AU} =& \mathbf{F_h} \\ [\mathbf{B}]_{i,j} =& \int_{\Gamma_h} \phi_j \phi_i \ \mathrm{d}\sigma_h, \\ [\mathbf{A}]_{i,j} =& \int_{\Gamma_h} \nabla_{\Gamma_h}\phi_j \cdot \nabla_{\Gamma_h}\phi_i \ \mathrm{d}\sigma_h, \\ [\mathbf{U}]_i =& U_i, \\ [\mathbf{F_h}]_j =& \int_{\Gamma_h} f_h \phi_j \ \mathrm{d}\sigma_h.\end{aligned} \tag{4.11}$$

B is called the **mass matrix** and **A** is the stiffness matrix. We point out that **A** and **B** are symmetric positive definite matrices.

4.2.5 Ritz projection

We define the **Ritz projection**, also known as the **elliptic projection**, $\pi_e : H_0^1(\Gamma) \to S_h(\Gamma_h)$ to satisfy the equation

$$a_h(\pi_e w, \chi) := a(w, \chi^\ell), \ \forall\ \chi \in S_h, \ \text{for } w \in H_0^1(\Gamma). \tag{4.12}$$

(cf. [56] equation (1.22) or [41] equation (2.1) for the flat surface case).

4.2.6 Elliptic Reconstruction

For a given Γ and Γ_h define the elliptic reconstruction $\hat{u} = \mathcal{R}u_h \in H_0^1(\Gamma)$ to be such that

$$a(\hat{u}, v) = (\mu_h^{-1}(A_h u_h - f_h)^\ell, v) + (f, v), \ \forall\ v \in H^1(\Gamma). \tag{4.13}$$

Define

$$g(t) := \mu_h^{-1}(A_h u_h - f_h)^\ell + f, \tag{4.14}$$

and

$$g_h(t) := A_h u_h. \tag{4.15}$$

Then

$$\mu_h g^\ell - g_h = \mu_h f^\ell - f_h. \tag{4.16}$$

It follows directly from (4.13) that

$$-\triangle_\Gamma \hat{u}(t) = g(t). \tag{4.17}$$

Remark Equations (4.12), (4.13) and (4.15) imply that for an equivalence class of functions $\pi_e^{-1}u_h \in \mathbf{H}_0^1(\Gamma)$ the following equation holds

$$a(\hat{u}, \chi^\ell) = a(\pi_e^{-1}u_h, \chi^\ell) + (\mu_h f^\ell - f_h, \chi)_h, \ \forall\ \chi \in S_h \tag{4.18}$$

i.e., modulo a geometric term $(\mu_h f^\ell - f_h, \chi)_h$ that goes to zero as $\Gamma_h \to \Gamma$, the Ritz

projection of the elliptic reconstruction $\hat{u}$ is the finite element solution u_h of the elliptic equation

$$\begin{cases} -\triangle_\Gamma u = g, & \text{on } \Gamma, \\ u = 0, & \text{in } \partial\Gamma. \end{cases} \tag{4.19}$$

Equation (4.19) allows us to apply the elliptic error estimates proved in Chapter 3 to prove our parabolic bounds.

4.3 A posteriori error bound

We now proceed to prove an a posteriori error bound (4.38) with similar structure to (4.1). Before proving the a posteriori bound we state and prove Lemmas 4.3.1, 4.3.2 and 4.3.3. We follow a similar argument to one presented in [41] for domains in $\mathbb{R}^n$.

Definition. For $s \geq 1$ and $v \in L^2(\Omega)$, we define the negative norm

$$\|v\|_{H^{-s}(\Omega)} = \sup_{w \in H^s(\Omega) \cap H_0^1(\Omega)} \frac{(v, w)}{\|w\|_{H^s(\Omega)}} \tag{4.20}$$

(cf. [56], [29])

Lemma 4.3.1 *Let u be the solution of (4.2) and $\hat{u}$ be the elliptic reconstruction defined as in (4.13). Then for all $t \in [0, T]$*

$$\begin{aligned} \|(\hat{u} - u)(t)\|^2_{L^2(\Gamma)} \leq & \|(\hat{u} - u)(0)\|^2_{L^2(\Gamma)} \\ & + \int_0^t \left\{ \|(\hat{u} - u_h^\ell)_\tau\|^2_{H^{-1}(\Gamma)} + \|(1 - \mu_h^{-1}) u_{h,\tau}^\ell\|^2_{H^{-1}(\Gamma)} \right\} d\tau \end{aligned} \tag{4.21}$$

Proof In the following discussion we use $A := -\triangle_\Gamma$ to denote the elliptic operator. It follows from (4.13) that

$$\begin{aligned} A\hat{u} =& \mu_h^{-1}(A_h u_h - f_h)^\ell + f \\ =& \mu_h^{-1}(-u_{h,t}^\ell) + f. \end{aligned}$$

Adding $(\hat{u} - u)_t$ to both sides of the previous equation and using $Au = f - u_t$ we get

$$(\hat{u} - u)_t + A(\hat{u} - u) = (\hat{u} - u_h^\ell)_t + (1 - \mu_h^{-1}) u_{h,t}^\ell.$$

We proceed with an energy argument. Multiplying by $(\hat{u} - u)$ on both sides of the last equation yields

$$(\hat{u} - u)_t(\hat{u} - u) + A(\hat{u} - u)(\hat{u} - u) = \left[(\hat{u} - u_h^\ell)_t + (1 - \mu_h^{-1}) u_{h,t}^\ell \right] (\hat{u} - u). \tag{4.22}$$

We then integrate in time and space and insert (4.22) to obtain

$$\begin{aligned}\int_\Gamma \int_0^t \left\{ \frac{1}{2}\frac{\partial}{\partial \tau}(\hat{u}-u)^2 + A(\hat{u}-u)(\hat{u}-u) \right\} \, d\tau \, \, \mathrm{d}\sigma \\ = \int_\Gamma \int_0^t \left\{ (\hat{u}-u_h^\ell)_\tau (\hat{u}-u) + (1-\mu_h^{-1}) u_{h,\tau}^\ell (\hat{u}-u) \right\} \, d\tau \, \, \mathrm{d}\sigma.\end{aligned} \tag{4.23}$$

Observe that $\int_\Gamma A(\hat{u}-u)(\hat{u}-u) \, \, \mathrm{d}\sigma = \int_\Gamma \nabla_\Gamma(\hat{u}-u)\cdot\nabla_\Gamma(\hat{u}-u) = \|(\hat{u}-u)\|^2_{H^1(\Gamma)}$. Then

$$\begin{aligned}\frac{1}{2}\left(\|(\hat{u}-u)(t)\|^2_{L^2(\Gamma)} - \|(\hat{u}-u)(0)\|^2_{L^2(\Gamma)} \right) + \int_0^t \|\hat{u}-u\|^2_{H^1(\Gamma)} \, d\tau \\ = \int_\Gamma \int_0^t \left\{ (\hat{u}-u_h^\ell)_\tau (\hat{u}-u) + (1-\mu_h^{-1}) u_{h,\tau}^\ell (\hat{u}-u) \right\} \, d\tau \, \, \mathrm{d}\sigma.\end{aligned} \tag{4.24}$$

Next we apply Hölder's and Cauchy's inequalities to obtain

$$\begin{aligned}&\frac{1}{2}\left(\|(\hat{u}-u)(t)\|^2_{L^2(\Gamma)} - \|(\hat{u}-u)(0)\|^2_{L^2(\Gamma)} \right) + \int_0^t \|\hat{u}-u\|^2_{H^1(\Gamma)} \, d\tau \\ &\leq \int_0^t \|(\hat{u}-u_h^\ell)_\tau\|_{H^{-1}(\Gamma)} \|\hat{u}-u\|_{H^1(\Gamma)} \, d\tau \\ &\quad + \int_\Gamma \|(1-\mu_h^{-1}) u_{h,\tau}^\ell\|_{H^{-1}(\Gamma)} \|\hat{u}-u\|_{H^1(\Gamma)} \, d\tau \\ &\leq \frac{1}{2}\int_0^t \left\{ \|(\hat{u}-u_h^\ell)_\tau\|^2_{H^{-1}(\Gamma)} + \|(1-\mu_h^{-1}) u_{h,\tau}^\ell\|^2_{H^{-1}(\Gamma)} \right\} \\ &\quad + \int_\Gamma \|\hat{u}-u\|^2_{H^1(\Gamma)} \, d\tau.\end{aligned} \tag{4.25}$$

The result follows after simplification and reordering, and noting that $\int_0^t \|\hat{u}-u\|^2_{H^1(\Gamma)} \geq 0$.

Lemma 4.3.2 *Let $\hat{u}$ be the elliptic reconstruction of u_h given by (4.13), $m=2$ for $deg(S_h)=1$ and $m=3$ for $deg(S_h)\geq 2$, and define*

$$\begin{aligned}\mathcal{E}_{H^{-1}}(\tau) :=& \|([P-\mathbf{A}_h^\ell]\nabla_\Gamma u_h^\ell)_\tau\|_{L^2(\Gamma)} + \Bigg(\sum_{T\in\mathcal{T}} \Big\{ h_T^{2m} \|(\mu_h g^\ell + \triangle_{\Gamma_h} u_h)_\tau\|^2_{L^2(T)} \\ &+ \|(\mu_h f^\ell - f_h)_\tau\|^2_{L^2(T)} + h_T^{2m-1} \|[\![\nabla_{\Gamma_h} u_{h,\tau}]\!]\|^2_{L^2(\partial T)} \Big\} \Bigg)^{1/2}.\end{aligned} \tag{4.26}$$

Then the following inequality holds for all $\tau\in[0,T]$

$$\|(\hat{u}-u_h^\ell)_\tau\|_{H^{-1}(\Gamma)} \lesssim \mathcal{E}_{H^{-1}}(\tau). \tag{4.27}$$

Proof By definition

$$\|(\hat{u}-u_h^\ell)_\tau\|_{H^{-1}(\Gamma)} := \sup_{\Psi\in H^1(\Gamma)}\left\{\frac{((\hat{u}-u_h^\ell)_\tau,\Psi)}{\|\Psi\|_{H^1(\Gamma)}}\right\}. \tag{4.28}$$

Let $\Psi\in H^1(\Gamma)$, and consider v such that

$$-\triangle_\Gamma v = \Psi. \tag{4.29}$$

Applying (4.29) and integration by parts to (4.28), we get

$$\frac{((\hat{u}-u_h^\ell)_\tau,\Psi)}{\|\Psi\|_{H^1(\Gamma)}} = \frac{(\nabla_\Gamma(\hat{u}-u_h^\ell)_\tau,\nabla_\Gamma v)}{\|\Psi\|_{H^1(\Gamma)}}.$$

We use equations (4.17) and (3.14) to get

$$\begin{aligned}((\hat{u}-u_h^\ell)_\tau,\Psi) =& \int_{\Gamma_h}(\mu_h g^\ell+\triangle_{\Gamma_h}u_h)_\tau(v^\ell-v_h)\ \mathrm{d}\sigma_h\\ &-\int_\Gamma([P-\mathbf{A}_h^\ell]\nabla_\Gamma u_h^\ell)_\tau\nabla_\Gamma v\quad \mathrm{d}\sigma\\ &+\int_{\Gamma_h}(\mu_h g^\ell-g_h)_\tau v_h\quad \mathrm{d}\sigma_h\\ &-\frac{1}{2}\sum_{T\in\mathcal{T}}\int_{\partial T}[\![\nabla_{\Gamma_h}u_h]\!]_\tau(v^\ell-v_h)\ \mathrm{d}s,\\ =&I+II+III+IV.\end{aligned} \tag{4.30}$$

We apply a similar argument to the one used to get the inequalities (3.18) through (3.22), with the difference that now $\deg(S_h)\in\{1,2\}$. The corresponding bounds for I, II, III and IV are

Bound for I. We repeat the argument used on (3.16) and (3.17) with the difference that now we use (2.32b) with $p=s=2$, $m=2$ for $\deg(S_h)=1$ and $m=3$ for $\deg(S_h)=2$. This yields

$$I\lesssim\left(\sum_{T\in\mathcal{T}}h_T^{2m}\|(\mu_h g^\ell+\triangle_{\Gamma_h}u_h)_\tau\|_{L^2(T)}\right)^{1/2}\|v\|_{H^m(\Gamma)}. \tag{4.31}$$

Bound for II. We repeat the argument used to derive the bound (3.19), but exchanging $\|v\|_{H^2(\Gamma)}$ for $\|v\|_{H^m(\Gamma)}$, to obtain

$$II\lesssim\left\{\sum_{T\in\mathcal{T}}\|[(\mathbf{P}-\mathbf{A}_h^\ell)\triangle_\Gamma u_h^\ell]_\tau\|^2_{L^2(a(T))}\right\}^{1/2}\|v\|_{H^m(\Gamma)}. \tag{4.32}$$

Bound for III. By the same argument used in (3.22) we write

$$III \lesssim \left(\sum_{T\in\mathcal{T}} \|(\mu_h g^\ell - g_h)_\tau\|^2_{L^2(T)} \right)^{1/2} \|v\|_{H^m(\Gamma)}. \tag{4.33}$$

Bound for IV. We repeat the argument used in (3.20), except that when we apply (2.32a) we pick $p = s = 2$, $m = 2$ for $\deg(S_h) = 1$ and $m = 3$ for $\deg(S_h) = 2$ to obtain

$$IV \lesssim \left(\sum_{T\in\mathcal{T}} h_T^{2m-1} \|[\![\nabla_{\Gamma_h} u_h]\!]_\tau\|^2_{L^2(\partial T)} \right)^{1/2} \|v\|_{H^m(\Gamma)}. \tag{4.34}$$

After combining equations (4.30) through (4.34) and using (4.16) it follows that

$$\begin{aligned}((\hat{u} - u_h^\ell)_\tau, \Psi) \lesssim \Bigg(& \|[P - \mathbf{A}_h^\ell]\nabla_\Gamma u_{h,\tau}^\ell\|_{L^2(\Gamma)} \\ & + \sqrt{\sum_{T\in\mathcal{T}} h_T^{2m} \|\mu_h g_\tau^\ell + \triangle_{\Gamma_h} u_{h,\tau}\|^2_{L^2(T)}} \\ & + \sqrt{\sum_{T\in\mathcal{T}} \|\mu_h f_\tau^\ell - f_{h,\tau}\|^2_{L^2(T)}} \\ & + \sqrt{\sum_{T\in\mathcal{T}} h_T^{2m-1} \|[\![\nabla_{\Gamma_h} u_h]\!]_\tau\|^2_{L^2(\partial T)}} \Bigg) \|v\|_{H^m(\Gamma)}.\end{aligned} \tag{4.35}$$

Equation (4.27) follows from (4.35) after observing that $\sqrt{\sum_i a_i^2} + \sqrt{\sum_i b_i^2} + \sqrt{\sum_i c_i^2} \leq \sqrt{2}\sqrt{\sum_i \{a_i^2 + b_i^2 + c_i^2\}}$, and using a shift lemma $\|v\|_{H^3(\Gamma)} \leq C\|\Psi\|_{H^1(\Gamma)}$.

Lemma 4.3.3 *Let $u(x;t)$ be the solution to (4.2) and let $\hat{u}$ be the elliptic reconstruction defined by (4.13), and let $\mathcal{E}_{H^{-1}}(\tau)$ be defined as in (4.26). Then the following inequality holds for all $t \in [0,T]$*

$$\begin{aligned}\|(u - \hat{u})(t)\|^2_{L^2(\Gamma)} \leq & \|(\hat{u} - u)(0)\|^2_{L^2(\Gamma)} \\ & + \int_0^t \left\{ \mathcal{E}^2_{H^{-1}}(\tau) + \|(1 - \mu_h^{-1}) u_{h,\tau}^\ell\|^2_{L^2(\Gamma)} \right\} \, d\tau\end{aligned} \tag{4.36}$$

Proof The proof follows from Lemmas 4.3.1, 4.3.2, and the fact that $L^2(\Gamma) \subset H^{-1}(\Gamma)$.

Theorem 4.3.4 *Let $u \in H^1(\Gamma)$ be the solution of (4.2), let $u_h \in S_h$ be the finite*

element solution of (4.2)*, take* $\mathcal{E}_{H^{-1}}(\tau)$ *to be given by* (4.26)*, and define*[1]

$$\begin{aligned}\mathcal{E}_{L^2}(\tau) :=&\Bigg(\sum_{T\in\mathcal{T}} \Big\{ \|[P - \mathbf{A}_h^\ell]\nabla_\Gamma u_h^\ell(t)\|^2_{L^2(a(T))} + h_T^4 \|\mu_h g^\ell(t) + \triangle_{\Gamma_h} u_h(t)\|^2_{L^2(T)} \\ &+ \|\mu_h f^\ell(t) - f_h(t)\|^2_{L^2(T)} + h_T^3 \|[\![\nabla_{\Gamma_h} u_h(t)]\!]\|^2_{L^2(\partial T)} \Big\} \Bigg)^{1/2},\end{aligned} \tag{4.37}$$

Then the following bound holds for all $t \in [0,T]$

$$\begin{aligned}\|(u - u_h^\ell)(t)\|_{L^2(\Gamma)} \lesssim& \|(u - u_h^\ell)(0)\|_{L^2(\Gamma)} + \left(\int_0^t \|(1-\mu_h^{-1}) u_{h,\tau}^\ell\|^2_{L^2(\Gamma)}\, d\tau \right)^{1/2} \\ &+ \mathcal{E}_{L^2}(t) + \mathcal{E}_{L^2}(0) + \left(\int_0^t \mathcal{E}^2_{H^{-1}}(\tau)\, d\tau \right)^{1/2}.\end{aligned} \tag{4.38}$$

Proof We use the triangle inequality to write

$$\|u - u_h^\ell\|_{L^2(\Gamma)} \le \|u - \hat{u}\|_{L^2(\Gamma)} + \|\hat{u} - u_h^\ell\|_{L^2(\Gamma)}. \tag{4.39}$$

Because, modulo a geometric term, $\hat{u}$ is the Ritz projection of the finite element solution of the elliptic problem (4.19) we use the bounds proved in Section 3.2, and (4.16) to find

$$\begin{aligned}\|\hat{u} - u_h^\ell\|_{L^2(\Gamma)}(t) \lesssim& \Bigg(\sum_{T\in\mathcal{T}} \Big\{ \|[P - \mathbf{A}_h^\ell]\nabla_\Gamma u_h^\ell(t)\|^2_{L^2(a(T))} \\ &+ h_T^4 \|\mu_h g^\ell(t) + \triangle_{\Gamma_h} u_h(t)\|^2_{L^2(T)} \\ &+ \|\mu_h f^\ell(t) - f_h(t)\|^2_{L^2(T)} \\ &+ h_T^3 \|[\![\nabla_{\Gamma_h} u_h(t)]\!]\|^2_{L^2(\partial T)} \Big\} \Bigg)^{1/2}, \\ =& \mathcal{E}_{L^2}(t).\end{aligned} \tag{4.40}$$

It follows from (4.36) and $\sqrt{\sum_i a_i^2} \le \sum_i |a_i|$ that

$$\|(\hat{u} - u)(t)\|_{L^2(\Gamma)} \le \|(\hat{u} - u)(0)\|_{L^2(\Gamma)} + \int_0^t \left\{ \mathcal{E}_{H^{-1}}(\tau) + \|(1-\mu_h^{-1}) u_{h,\tau}^\ell\|_{L^2(\Gamma)} \right\} d\tau. \tag{4.41}$$

By the triangle inequality and (4.40) we get

$$\|(\hat{u} - u)(0)\|_{L^2(\Gamma)} \le \|(u - u_h^\ell)(0)\|_{L^2(\Gamma)} + \mathcal{E}_{L^2}(0). \tag{4.42}$$

[1] In contrast with (4.26) we use $m = 2$ to bound $\|\hat{u} - u_h^\ell\|_{L^2}$.

The result follows after combining (4.39), (4.40), (4.41), and (4.42).

Corollary 4.3.5 *Since* (4.38) *holds for all* $t \in [0,T]$ *it follows that*

$$\begin{aligned}\max_{0\leq t\leq T}\|(u-u_h^\ell)(t)\|_{L^2(\Gamma)} \lesssim & \|(u-u_h^\ell)(0)\|_{L^2(\Gamma)} \\ & + \left(\int_0^T \|(1-\mu_h^{-1})u_{h,\tau}^\ell\|_{L^2(\Gamma)}^2\, d\tau\right)^{1/2} \\ & + 2\max_{0\leq t\leq T}\mathcal{E}_{L^2}(t) + \left(\int_0^t \mathcal{E}_{H^{-1}}^2(\tau)\, d\tau\right)^{1/2}.\end{aligned} \tag{4.43}$$

Comparing equations (4.1) and (4.43) we see that they posses the same structure. The differences between flat and general surfaces are captured in the elliptic estimators $\mathcal{E}_{L^2}$, $\mathcal{E}_{H^{-1}}$, and the extra geometric term $\left(\int_0^T \|(1-\mu_h^{-1})u_{h,\tau}^\ell\|_{L^2(\Gamma)}^2\, d\tau\right)^{1/2}$.

4.3.1 Future work

The error estimate (4.38) is only discrete in space. To implement the results in this section one must carry out a time stepping procedure. The most immediate goal that we have is to use the preliminary results of this section to implement a fully discrete scheme solving (4.2).

We plan to carry out spatial adptivity every "few" steps using the results of this chapter. For the time marching scheme we propose to use Crank-Nicolson. An advantage of using Crank-Nicolson is that the time marching scheme obtained is unconditionally stable. Crank-Nicolson applied to (4.11) yields

$$U_t \approx \frac{\mathbf{U}^{(n+1)}-\mathbf{U}^{(n)}}{k} = \frac{-\mathbf{B}^{-1}\mathbf{A}\mathbf{U}^{(n+1)} + \mathbf{B}^{-1}{\mathbf{F_h}}^{(n+1)} - \mathbf{B}^{-1}\mathbf{A}\mathbf{U}^{(n)} + \mathbf{B}^{-1}{\mathbf{F_h}}^{(n)}}{2},$$

here k is the size of the time step. The super indexes $(n+1)$ and (n) denote the time steps $n+1$ and n respectively. Rearrangement of the previous expression gives

$$\left[\mathbf{B}+\frac{k}{2}\mathbf{A}\right]\mathbf{U}^{(n+1)} = \left[\mathbf{B}-\frac{k}{2}\mathbf{A}\right]\mathbf{U}^{(n)} + \frac{k}{2}[{\mathbf{F_h}}^{(n+1)} + {\mathbf{F_h}}^{(n)}]. \tag{4.44}$$

Observe that at step $(n+1)$ the right hand side of (4.44) is a known quantity. It depends solely on the solution $\mathbf{U}^{(n)}$ of the previous time step and the known load vector $\mathbf{F_h}(t)$. Thus (4.44) provides a, fully discrete, marching scheme that can be used to compute the numerical solution. We also point out that the matrix $\left[\mathbf{B}+\frac{k}{2}\mathbf{A}\right]$ is sparse symmetric positive definite; and the number of operations required to assemble the right hand side of (4.44) is $\mathcal{O}(N)$. We note that there are "fast" numerical algorithms available to solve (4.44).

Another goal that we have already discussed is to work with evolving surfaces, and applications to membranes (cf. [7], [31]) among others.

Bibliography

[1] Robert A. Adams and John J. F. Fournier, *Sobolev spaces*, vol. 140 of Pure and Applied Mathematics (Amsterdam), Elsevier/Academic Press, Amsterdam, second ed., 2003.

[2] Yonathan Aflalo, Ron Kimmel, and Michael Zibulevsky, *Conformal mapping with as uniform as possible conformal factor.*, SIAM J. Imaging Sciences, 6 (2013), pp. 78–101.

[3] Mark Ainsworth and J. Tinsley Oden, *A posteriori error estimation in finite element analysis*, Pure and Applied Mathematics (New York), Wiley-Interscience [John Wiley & Sons], New York, 2000.

[4] Douglas N. Arnold, Richard S. Falk, and Ragnar Winther, *Finite element exterior calculus: from Hodge theory to numerical stability*, Bull. Amer. Math. Soc. (N.S.), 47 (2010), pp. 281–354.

[5] Thierry Aubin, *Nonlinear analysis on manifolds. Monge-Ampère equations*, vol. 252 of Grundlehren der Mathematischen Wissenschaften [Fundamental Principles of Mathematical Sciences], Springer-Verlag, New York, 1982.

[6] Sören Bartels and Rüdiger Müller, *Quasi-optimal and robust a posteriori error estimates in $L^\infty(L^2)$ for the approximation of Allen-Cahn equations past singularities*, Math. Comp., 80 (2011), pp. 761–780.

[7] Dolzmann G. Bartels S., Nochetto R., *A finite element scheme for the evolution of orientational order in fluid membranes*, Math. Model. Numer. Anal, (2010), pp. 1–32.

[8] Andrea Bonito, J. Manuel Cascon, Pedro Morin, and Ricardo H. Nochetto, *AFEM for Geometric PDE: The Laplace-Beltrami Operator*, in Analysis and Numerics of Partial Differential Equations. In memory of Enrico Magenes, vol. 4 of Springer INdAM Series, Springer, 2013.

[9] Bramble and Hilbert, *Estimation of linear functionals on sobolev spaces with application to fourier transforms and spline interpolation*, SIAM J. Numer. Anal, 7 (1970).

[10] J. H. Bramble and S. R. Hilbert, *Bounds for a class of linear functionals with applications to Hermite interpolation*, 16 (1971), pp. 362–369.

[11] Susanne C. Brenner and L. Ridgway Scott, *The mathematical theory of finite element methods*, vol. 15 of Texts in Applied Mathematics, Springer, New York, third ed., 2008.

[12] F. Camacho and A. Demlow, *L_2 and pointwise a posteriori error estiamtes for FEM for elliptic PDE on surfaces*, IMA J. Numer. Anal., (2014).

[13] V. Carey, D. Estep, A. Johansson, M. Larson, and S. Tavener, *Blockwise adaptivity for time dependent problems based on coarse scale adjoint solutions*, SIAM J. Scientific Computing, 32 (2010), pp. 2121–2145.

[14] Long Chen, *iFEM: An innovative finite element method package in Matlab*, tech. report, Submitted.

[15] Philippe G. Ciarlet, *The finite element method for elliptic problems*, vol. 40 of Classics in Applied Mathematics, Society for Industrial and Applied Mathematics (SIAM), Philadelphia, PA, 2002. Reprint of the 1978 original [North-Holland, Amsterdam; MR0520174 (58 #25001)].

[16] U. Clarenz, U. Diewald, G. Dziuk, M. Rumpf, and R. Rusu, *A finite element method for surface restoration with smooth boundary conditions*, Comput. Aided Geom. Design, 21 (2004), pp. 427–445.

[17] R.W. Clough, *The Finite Element Method in Plane Stress Analysis*, American Society of Civil Engineers, 1960.

[18] R. Courant, *Variational methods for the solution of problems of equilibrium and vibratrions*, Trans. Amer. Math. Soc., 1-23 (1942).

[19] Alan Demlow, *Higher-order finite element methods and pointwise error estimates for elliptic problems on surfaces*, SIAM J. Numer. Anal., 47 (2009), pp. 805–827.

[20] Alan Demlow and Gerhard Dziuk, *An adaptive finite element method for the Laplace-Beltrami operator on implicitly defined surfaces*, SIAM J. Numer. Anal., 45 (2007), pp. 421–442 (electronic).

[21] Alan Demlow and Emmanuil Georgoulis, *Pointwise a posteriori error control for discontinuous Galerkin methods for elliptic problems*, SIAM J. Numer. Anal., 50 (2012), pp. 2159–2181.

[22] Alan Demlow, Omar Lakkis, and Charalambos Makridakis, *A posteriori error estimates in the maximum norm for parabolic problems*, SIAM J. Numer. Anal., 47 (2009), pp. 2157–2176.

[23] Alan Demlow and Maxim Olshanskii, *An adaptive surface finite element method based on volume meshes*, SIAM J. Numer. Anal., 50 (2012), pp. 1624–1647.

[24] Gerhard Dziuk, *Finite elements for the Beltrami operator on arbitrary surfaces*, in Partial differential equations and calculus of variations, vol. 1357 of Lecture Notes in Math., Springer, Berlin, 1988, pp. 142–155.

[25] G. Dziuk, *An algorithm for evolutionary surfaces*, Numer. Math., 58 (1991), pp. 603–611.

[26] G. Dziuk and C. Elliott, *Surface finite elements for parabolic equations*, J. Comput. Math., 25 (2007), pp. 385–407.

[27] G. Dziuk and C. M. Elliott, *Finite elements on evolving surfaces*, IMA J. Numer. Anal., 27 (2007), pp. 262–292.

[28] Kenneth Eriksson, *An adaptive finite element method with efficient maximum norm error control for elliptic problems*, Math. Models Methods Appl. Sci., 4 (1994), pp. 313–329.

[29] Alexandre Ern and Jean-Luc Guermond, *Theory and practice of finite elements*, vol. 159 of Applied Mathematical Sciences, Springer-Verlag, New York, 2004.

[30] Lawrence C. Evans, *Partial differential equations*, vol. 19 of Graduate Studies in Mathematics, American Mathematical Society, Providence, RI, 1998.

[31] Feng Feng and William S. Klug, *Finite element modeling of lipid bilayer membranes*, Journal of Computational Physics, 220 (2006), pp. 394–408.

[32] David Gilbarg and Neil S. Trudinger, *Elliptic Partial Differential Equations of Second Order*, Springer-Verlag, Berlin, 2nd ed., 1998.

[33] Sven Gross, Volker Reichelt, and Arnold Reusken, *A finite element based level set method for two-phase incompressible flows*, Comput. Vis. Sci., 9 (2006), pp. 239–257.

[34] Sven Gross and Arnold Reusken, *Finite element discretization error analysis of a surface tension force in two-phase incompressible flows*, SIAM J. Numer. Anal., 45 (2007), pp. 1679–1700 (electronic).

[35] Weizhang Huang and Robert D. Russell, *Adaptive moving mesh methods*, Applied mathematical sciences, Springer, New York, Heidelberg, London, 2011.

[36] L. Ju, Tian and D. Wang, *A posteriori error estimates for finite volume approximations of elliptic equations on general surfaces.*, Comput. Methods Appl. Mech. Engrg., 198 (2009), pp. 716–726.

[37] J.L. Meek K. K. Gupta, *A brief history of the beginning of the finite element method*, Journal for Numerical Methods in Engineering, 39 (1996), pp. 3761–3774.

[38] Natalia Kopteva and Torsten Linss, *Maximum norm a posteriori error estimation for parabolic problems using elliptic reconstructions*, SIAM J. Numerical Analysis, 51 (2013), pp. 1494–1524.

[39] Omar Lakkis and Charalambos Makridakis, *Elliptic reconstruction and a posteriori error estimates for fully discrete linear parabolic problems*, Math. Comp., 75 (2006), pp. 1627–1658 (electronic).

[40] Xiaohai Liao and Ricardo H. Nochetto, *Local a posteriori error estimates and adaptive control of pollution effects*, Numer. Methods Partial Differential Equations, 19 (2003), pp. 421–442.

[41] Charalambos Makridakis and Ricardo H. Nochetto, *Elliptic reconstruction and a posteriori error estimates for parabolic problems*, SIAM J. Numer. Anal., 41 (2003), pp. 1585–1594 (electronic).

[42] Khamron Mekchay, Pedro Morin, and Ricardo H. Nochetto, *AFEM for the Laplace-Beltrami operator on graphs: design and conditional contraction property*, Math. Comp., 80 (2011), pp. 625–648.

[43] Gary L. Miller, Dafna Talmor, and Shang-Hua Teng, *Optimal good-aspect-ratio coarsening for unstructured meshes*, 1997.

[44] Ricardo H. Nochetto, *Pointwise a posteriori error estimates for elliptic problems on highly graded meshes*, Math. Comp., 64 (1995), pp. 1–22.

[45] Ricardo H. Nochetto and Andreas Veeser, *Multiscale and adaptivity: modeling, numerics and applications*, Springer-Verlag, 2012, ch. Primer of Adaptive Finite Element Methods, pp. 125–226.

[46] Veeser A. Nochetto R. H., *Primer of adaptive finite element methods.* http://www2.math.umd.edu/ rhn/lectures/cime.pdf, 2009.

[47] T. Oden, *Some historic comments on finite elements*, in Proceedings of the ACM Conference on History of Scientific and Numeric Computation, HSNC '87, New York, NY, USA, 1987, ACM, pp. 125–130.

[48] Maxim A. Olshanskii, Arnold Reusken, and Jörg Grande, *A finite element method for elliptic equations on surfaces*, SIAM J. Numer. Anal., 47 (2009), pp. 3339–3358.

[49] P.-O. Persson and J. Peraire, *Curved mesh generation and mesh refinement using lagrangian solid mechanics*, (2008).

[50] Mathew Potter, *Anisotropic mesh coarsening and refinement on GPU architecture*, tech. report, Imperial College London, June 2011.

[51] Martin Reuter, Silvia Biasotti, Daniela Giorgi, Giuseppe Patanè, and Michela Spagnuolo, *Discrete Laplace-Beltrami operators for shape analysis and segmentation*, Computers & Graphics, 33 (2009), pp. 381–390.

[52] Martin Reuter, Franz-Erich Wolter, and Niklas Peinecke, *Laplace-Beltrami spectra as "shape-DNA" of surfaces and solids*, Computer-Aided Design, 38 (2006), pp. 342–366.

[53] L. Ridgway Scott and Shangyou Zhang, *Finite element interpolation of nonsmooth functions satisfying boundary conditions*, Math. Comp., 54 (1990), pp. 483–493.

[54] E. Stein, R. de Borst, and T.J.R. Hughes, *Encyclopedia of computational mechanics*, no. v. 1 in Encyclopedia of Computational Mechanics, John Wiley, 2004.

[55] Gilbert Strang and George J. Fix, *An Analysis of the Finite Element Method*, Prentice-Hall, Inc., Englewood Cliffs, NJ, 1973.

[56] V. Thomée, *Galerkin Finite Element Methods for Parabolic Problems*, Springer series in computational mathematics, Springer, 2010.

[57] Joe F. Thompson, Bharat K. Soni, and Nigel P. Weatherhill, eds., *Handbook of Grid Generation*, CRC Press, 1999.

[58] A. Veeser, *Local and global approximation of gradients with piecewise polynomial functions*, tech. report, Università degli Studi di Milano, 2013.

[59] R. Verfürth, *A posteriori error estimation and adaptive mesh-refinement techniques*, in Proceedings of the Fifth International Congress on Computational and Applied Mathematics (Leuven, 1992), vol. 50, 1994, pp. 67–83.

[60] Huang Y. Wei H., Chen L., *Superconvergence and gradient recovery of linear finite elements for the laplace-beltrami operator on general surfaces.*, SIAM J. Numer. Anal, 48 (2010), pp. 1920–1943.

[61] Aaron Wetzler, Yonathan Aflalo, Anastasia Dubrovina, and Ron Kimmel, *The Laplace-beltrami operator: a ubiquitous tool for image and shape processing.* Hendriks, Cris L. Luengo (ed.) et al., Mathematical morphology and its applications to signal and image processing. 11th international symposium, ISMM 2013, Uppsala, Sweden, May 27–29, 2013. Proceedings. Berlin: Springer. Lecture Notes in Computer Science 7883, 302-316 (2013)., 2013.

[62] Thomas P. Wihler, *Weighted L^2-norm a posteriori error estimation of FEM in polygons*, Int. J. Numer. Anal. Model., 4 (2007), pp. 100–115.

Index

U

V

W

Brief Curriculum Vitae

Fernando Faustino Camacho

Education

- Instituto Tecnológico y de Estudios Superiores de Monterrey.
    - B.S. Mechanical and Electrical Engineering, May 2001.

Publications

- *L_2 and pointwise a posteriori error estimates for FEM for elliptic PDE on surfaces.,* IMA Journal of Numerical Analysis (Accepted July 2014).

Posters

- *A posteriori error estimates for elliptic PDE on surfaces.*, Blackwell-Tapia conference 2012, ICERM Providence RI.
- *A posteriori error estimates for FEM on Surfaces.*, SACNAS National conference, Seattle WA.

Professional Experience

- Teaching Assistant, University of Kentucky, Lexington Kentucky, January 2007 to present
- New Projects Assistant Manager, Controladora Comercial Mexicana, D.F. México, September 2004 - March 2006.
- Proposals Chief, Duro Felguera, D.F. México, December 2001 - July 2004.